

Engineering Asymmetry: Geometric Design of Nanoscale Lipid Vesicles for Uptake-Optimized Drug Delivery

A thesis presented by

Shahmir Aziz

to the

Harvard John A. Paulson School of Engineering and Applied Sciences
and the Department of Mathematics

in partial fulfillment of the requirements for
the Bachelor of Arts degree with honors in
Biomedical Engineering and Mathematics

Faculty Adviser: Prof. David Weitz

Harvard University

Cambridge, MA

March 25, 2025

Harvard Honor Code

In submitting this thesis to the Harvard John A. Paulson School of Engineering and Applied Sciences in partial fulfillment of the requirements for the degree with honors of Bachelor of Arts, I affirm my awareness of the standards of the Harvard College Honor Code.

Name: *Shahmir Aziz*

A handwritten signature in black ink, appearing to read "Shahmir Aziz".

The Harvard College Honor Code Members of the Harvard College community commit themselves to producing academic work of integrity – that is, work that adheres to the scholarly and intellectual standards of accurate attribution of sources, appropriate collection and use of data, and transparent acknowledgment of the contribution of others to their ideas, discoveries, interpretations, and conclusions. Cheating on exams or problem sets, plagiarizing or misrepresenting the ideas or language of someone else as one's own, falsifying data, or any other instance of academic dishonesty violates the standards of our community, as well as the standards of the wider world of learning and affairs.

Contents

List of Figures	6
1 Drug Delivery and the Promise of Lipid Vesicles – Introduction	2
1.1 Drug Delivery	3
1.1.1 Therapeutics and Administration	3
1.1.2 Challenges in Direct Drug Administration	3
1.1.3 The Importance of Drug Delivery Systems	4
1.1.4 Current Landscape of Drug Delivery Vehicles	5
1.2 Asymmetric Lipid Vesicles as an Emerging Drug Delivery Platform	8
1.2.1 Hypothesis	8
1.2.2 A Roadmap to Asymmetric Vesicles	10
1.2.3 Challenges and Unknowns	11
1.2.4 Thesis Goals	14
1.2.5 Thesis Outline	15
2 Geometric and Symmetric Analysis of Lipid Vesicles	16
2.1 Introduction	17
2.2 Mathematical Foundations	18
2.2.1 Differential Geometry of Surfaces	18
2.2.2 Helfrich Energy and Bending Rigidity	20
2.2.3 Membrane Tension and Area Expansion	23

2.2.4	Spontaneous Curvature and Asymmetry	24
2.3	Measurable Geometric Properties and Theoretical Interpretation	26
2.3.1	Membrane Fluidity and Laurdan GP	26
2.3.2	Surface Charge and Zeta Potential	27
2.3.3	Micropipette Aspiration and Bending Modulus	28
2.4	Perspective	29
3	Designing and Testing the Lipid Vesicle – Methods	30
3.1	Designing the Vesicle	31
3.1.1	Bi-leaflet Lipid Vesicles	31
3.1.2	Lipid Composition Permutations	31
3.1.3	Vesicle Engineering Technique	34
3.2	Testing Vesicle Performance and Characteristics	35
3.2.1	Membrane Fluidity	35
3.2.2	Zeta Potential for Chemical Asymmetry	37
3.2.3	Uptake Measurement	37
4	Results	41
4.1	Symmetric vs Asymmetric Vesicles	42
4.2	Zeta Potential and Cellular Uptake	44
4.3	Membrane Fluidity (GP) and Cellular Uptake	46
4.4	Multi-Parameter Correlation	47
4.5	Summary of Observations	48
5	Bridging the Empirical and the Theoretical – Discussion	49
5.1	Asymmetry-Induced Uptake and Spontaneous Curvature	50
5.2	Electrostatics and the Effective Bending Modulus	52
5.3	Membrane Fluidity, Bending Rigidity, and Curvature Coupling	54
5.4	Correlated Effects: Toward a Unified Model	55

5.5 Perspective	56
5.5.1 Limitations	56
5.5.2 Future Direction	56
6 Conclusion	58
6.0.1 Theoretical Unification and Implications	59
6.0.2 Broader Context: Toward Universal Drug Delivery Systems	59
6.0.3 Final Remarks	60
A Experimental Section	62
Bibliography	65

List of Figures

1.1	Encapsulation of packages by Lipid Vesicles	10
1.2	Endocytosis – Uptake Methodology of Vesicles by Cells	12
3.1	Asymmetric and Symmetric Nanoscale Lipid Vesicles	32
3.2	Engineering Method of Lipid Vesicles	34
3.3	Emission Shifts of Vesicles Using Laurdan	35
3.4	Example of Fluorescence Images Using POPC/EPC Vesicles. The left image shows just the fluorescence, while the right image shows the composite image of fluorescence and Brightfield imaging. The intensity of the red dye is correlated with the quantity of vesicles that were taken up by the cells being imaged.	40
4.1	Uptake (Fluorescence Intensity) of Asymmetric and Symmetric Vesicles . . .	42
4.2	Asymmetric Vesicle Uptake Compared to Symmetric Counterparts for EPC (Cationic) and POPS (Anionic) Lipids.	43
4.3	Scatterplot of Zeta Potential Values with Uptake (Measured through Fluorescence Intensity)	44
4.4	Scatterplot of Membrane Fluidity (GP) with Uptake	46

4.5 Heatmap visualization of the relationship between Zeta Potential (mV), Generalized Polarization, and Uptake. Color intensity represents interpolated Uptake values (a.u.) across the Zeta-GP parameter space, with greater intensity indicating higher Uptake. The continuous surface is generated using cubic interpolation of experimental data points spanning both positive and negative Zeta Potential ranges.	47
5.1 Curvature of different lipid structures	51

Abstract

It is often the case that therapeutics needed to treat particular diseases or ailments cannot be administered directly into the bloodstream or digestive system. Due to problems like toxicity in non-targeted environments or requirements for higher uptake by target cells, they often need to be transported by drug delivery vehicles. Today, a broad range of such vehicles are used, including Lipid NanoParticles (LNPs) and Viral Vectors, but they all face significant shortcomings (in this case, limited parameter space for packaging only negatively charged molecules, and size constraint of packages respectively).

We explore a new type of drug delivery system, namely nanoscale bi-leaflet lipid vesicles, which have shown promise in encapsulating a large set of drugs without size or charge constraints. The biggest challenge currently facing lipid vesicles is limited cellular uptake, which we explore in this thesis through a geometric and symmetric lens. We show that asymmetry between the inner and outer leaflet of the vesicles enhances uptake by up to 9-fold in some cases, while showing that higher magnitudes of zeta potential and greater membrane fluidity enhance uptake as well. We also relate these empirical findings to geometric theory to synthesize our learnings and move toward an optimization model to maximize vesicle uptake by cells.

This research hopes to contribute to forming more efficient, universal drug carriers and make it possible to transport therapeutics never delivered before, including the CRISPR Cas-9 gene-editing protein among other large, complex proteins and drugs.

Chapter 1

Drug Delivery and the Promise of Lipid Vesicles – Introduction

The future of medicine lies in targeted therapy: not in killing everything, but in precision.

SIDDHARTHA MUKHERJEE

We will begin this thesis by setting the scope of the research and outlining the need for the drug delivery space along with its challenges today, before delving into an overview of our proposed solution to expand the parameter space of transportable drugs – asymmetric, bi-leaflet nanoscale lipid vesicles.

1.1 Drug Delivery

1.1.1 Therapeutics and Administration

The use of therapeutics has been a cornerstone of medicine for centuries, evolving from crude natural extracts to sophisticated, molecularly targeted drugs. Chronic illnesses such as cancer, diabetes, cardiovascular diseases, and infectious diseases pose significant global health burdens and drive the ongoing need for new and improved therapeutic agents [1], and advancements in molecular biology and genomics have led to the emergence of precision medicine, necessitating highly specific drug formulations tailored to individual patients.

The pharmaceutical industry is continuously developing, and advances in pharmacology and molecular biology have produced a wide array of small molecules, nucleic acids, proteins, and gene-editing tools such as *CRISPR-Cas9*, each with unique chemical properties and therapeutic potential. However, the mere discovery of effective drugs is only one piece of the treatment puzzle – the second half of the challenge of modern therapeutics is ensuring that the designed drugs reach the intended location in the body in optimal concentrations while minimizing systemic toxicity and side effects. This necessity underscores the importance of drug delivery systems, which enhance the pharmacokinetics, bioavailability, and therapeutic index of drugs [2].

1.1.2 Challenges in Direct Drug Administration

Traditional methods of drug administration, including oral ingestion, intravenous injection, and inhalation, come with inherent limitations.¹ For orally administered drugs, bioavailability is often compromised due to enzymatic degradation in the gastrointestinal tract and first-pass metabolism in the liver, leading to reduced drug concentrations reaching systemic circulation [3]. Similarly, intravenously injected drugs, while bypassing first-pass

¹Intravenous injection refers to the drug solution being injected directly into the vein with the intention of it reaching the target cells through normal blood flow

metabolism, may suffer from rapid clearance, poor tissue penetration, and systemic toxicity due to nonspecific biodistribution.

For instance, chemotherapy agents used to treat cancer often exhibit significant off-target toxicity, affecting healthy tissues and causing severe side effects such as immunosuppression, nausea, and organ damage [4]. Similarly, antibiotics administered systemically can disrupt the gut microbiome, leading to antibiotic resistance and secondary infections. These challenges highlight the urgent need for controlled drug delivery systems that can enhance specificity, prolong circulation time, and optimize therapeutic efficacy.

1.1.3 The Importance of Drug Delivery Systems

Drug delivery systems aim to optimize the absorption, distribution, metabolism, and excretion (ADME) properties of therapeutics, ensuring that drugs reach their targets effectively while minimizing unwanted effects. The development of advanced drug delivery mechanisms has enabled the following:

- **Targeted Therapy:** By directing drugs to specific cells, tissues, or organs, targeted delivery systems can significantly reduce off-target effects and enhance therapeutic outcomes. This is particularly important in oncology, where tumor-targeted drug carriers improve treatment efficacy while minimizing toxicity [5].
- **Controlled Release:** Many drugs require sustained or controlled release profiles to maintain therapeutic concentrations over time. Polymeric nanoparticles, liposomes, and hydrogels have been developed to enable controlled drug release, reducing the frequency of administration and improving patient compliance [6].
- **Protection from Degradation:** Biologic drugs, including peptides, proteins, and nucleic acids, are highly susceptible to enzymatic degradation. Encapsulation within protective carriers, such as lipid vesicles, can enhance stability and extend the half-life of these therapeutics in circulation [7].

- **Improved Solubility and Bioavailability:** Poor water solubility is a major hurdle in drug formulation, limiting the absorption of many potent therapeutic molecules. Nanocarriers, surfactants, and lipid-based formulations can enhance solubility and bioavailability, making previously ineffective drugs viable for clinical use [8].

1.1.4 Current Landscape of Drug Delivery Vehicles

Here we briefly overview some of the existing drug delivery mechanisms in today's status quo, outlining their main benefits as well as drawbacks which limit their parameter space or throughput. This is to contextualize the gap that we project lipid vesicles can fill, and set the scope of the alternatives present. This is by no means an exhaustive list, but aims to go over the central vehicles driving the industry as of today.

Lipid Nanoparticles (LNPs)

Lipid nanoparticles (LNPs) have gained widespread recognition as effective delivery vehicles for nucleic acids, particularly in the context of mRNA vaccines for COVID-19 [9]. LNPs typically consist of four major components: ionizable lipids (which facilitate endosomal escape), phospholipids (providing structural stability), cholesterol (enhancing membrane fusion), and polyethylene glycol (PEG) lipids (improving circulation time). The success of LNPs in nucleic acid delivery is largely due to their ability to encapsulate negatively charged mRNA and protect it from enzymatic degradation [10].

However, despite their advantages, LNPs face several limitations. One major challenge is their reliance on electrostatic interactions for encapsulation, making them less effective for neutral or positively charged biomolecules such as proteins [11]. This translates to a limited parameter space for the type of drugs that LNPs can act as vehicles for. Additionally, LNPs can elicit immune responses, and their biodistribution is often restricted to the liver due to uptake by hepatocytes [12].

Viral Vectors

Viral vectors, such as adeno-associated viruses (AAVs) and lentiviruses, have been extensively used in gene therapy applications [13]. These vectors leverage the natural ability of viruses to enter cells and deliver genetic material efficiently. AAVs, in particular, have been used to treat genetic disorders by introducing functional copies of defective genes [14].

Despite their high efficiency, viral vectors face several drawbacks. The primary concern is immunogenicity, as pre-existing immunity to viral capsids can reduce transduction efficiency and lead to adverse reactions [15]. Additionally, viral vectors have a fixed genome size capacity, limiting their ability to carry large therapeutic genes [16]. This is particularly hindering when aiming to transport large molecules such as proteins to target cells, which is the case in many modern drug development techniques, including *CRISPR*'s *Cas9* protein. Manufacturing complexities and high production costs further hinder their widespread adoption.

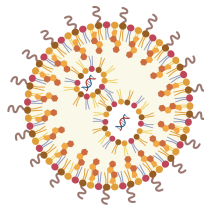
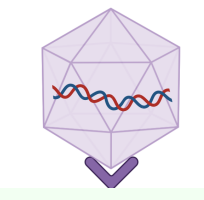
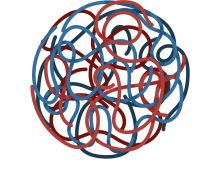
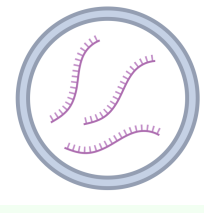
Polymeric Nanoparticles

These synthetic carriers offer tunable physicochemical properties for drug delivery. Polymers such as poly(lactic-co-glycolic acid) (PLGA) enable sustained release but face challenges related to toxicity and degradation byproducts [17].

Extracellular Vesicles (EVs)

EVs, including exosomes, represent an emerging class of drug carriers derived from cell membranes. They offer innate biocompatibility and targeting capabilities but suffer from low production yields and complex isolation processes [18].

Table 1.1: Comparison of Prominent Drug Delivery Vehicles

Delivery System	Weaknesses / Drawbacks
Lipid Nanoparticles (LNPs)	 <p>Limited to negatively charged molecules; restricted biodistribution (primarily liver); immune activation risk.</p>
Viral Vectors	 <p>Immunogenicity; limited packaging capacity; expensive manufacturing; regulatory challenges.</p>
Polymeric Nanoparticles	 <p>Potential toxicity; degradation byproducts; complex synthesis; stability concerns.</p>
Extracellular Vesicles (EVs)	 <p>Low production yield; complex isolation/purification; heterogeneity; scalability issues.</p>

1.2 Asymmetric Lipid Vesicles as an Emerging Drug Delivery Platform

1.2.1 Hypothesis

Given the constraints described in the previous subsection which are attached to status quo alternatives, particularly the constraint of packaging drugs of all charges (as is a problem with LNPs), and the constraint of packaging larger molecules (as is a problem with viral vectors, which can only fit packages as large as the viral vector being used, which is hard to finetune or alter artificially), we set out to find an alternative which expands the parameter space of drugs that can be delivered, both in terms of size and charge.

Lipid vesicles are *bilayered spherical compartments composed of amphiphilic lipids*. The vesicle contains an inner leaflet made of one lipid, which is exposed to the package being delivered, and an outer leaflet, potentially made from a different lipid composition, which is exposed to the surroundings in the body, and which interacts with the cell membranes of the cells being targeted.

Particularly, our research focuses on *asymmetric lipid vesicles*, where the inner and outer leaflets of the bilayer are compositionally distinct [16]. This departure from conventional symmetric designs is driven by the recognition that **biological membranes themselves are inherently asymmetric**, with differences in lipid composition influencing cellular interactions, membrane fluidity, and fusion events. As a result, asymmetric vesicles hold the potential to enhance membrane fusion, regulate drug release kinetics, and improve cellular uptake mechanisms in ways that symmetric vesicles cannot achieve.

Unlike LNPs, lipid vesicles are not limited by electrostatic interactions and can encapsulate a much broader range of therapeutic agents, including proteins, nucleic acids, and hydrophobic drugs, as they do not depend on electrostatic interactions to package their desired drugs [19]. The idea is that lipid vesicles serve as a '*water in oil*' droplet, with the

lipids surrounding an aqueous solution inside. Given that most drugs are soluble in water, this allows the packaging of a very diverse set of molecules, and for drugs which are not soluble in water, the solution packaged by the lipid leaflets can be altered as is required. The tunable size of the vesicles also means that we can design vesicles based on the need of the molecule being packaged, which can include larger molecules including the *CRISPR-Cas9* protein, which we have tested in our lab and can be adequately packaged by aforementioned vesicles.

A key advantage of lipid vesicles is their ability to be engineered with specific lipid compositions – these different lipid compositions also mean that we can package a larger set of drugs, as some might not interact favorably with a particular lipid but do not adversely react with a differently charged lipid.

The incorporation of targeting ligands or surface modifications (e.g., PEGylation or polysaccharide functionalization) can further enhance their specificity and reduce clearance by the immune system [12]. This added specificity ensures that the targeted delivery of particular sensitive or potentially harmful drugs can be undertaken with tailor-made attachments and modifications on the surface of the vesicle.

Our lab has already conducted research to show successful compartmentalization of a diverse set of packages, ranging from CRISPR-Cas9 to antibodies to mRNA, and thus it is established that these vesicles can adequately contain within themselves a very broad set of drugs.

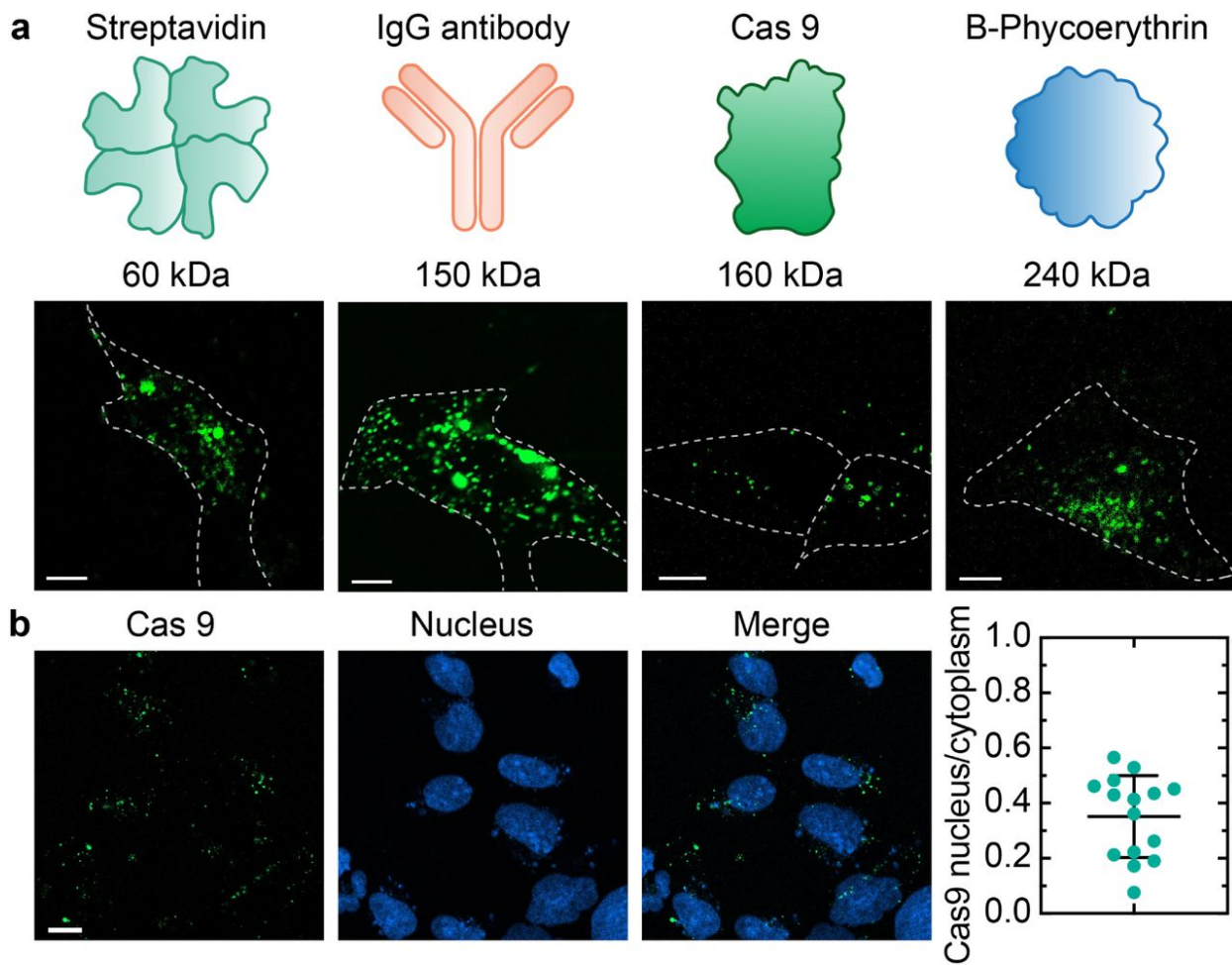


Figure 1.1: Encapsulation of packages by Lipid Vesicles

1.2.2 A Roadmap to Asymmetric Vesicles

Lipid vesicles have played a pivotal role in drug delivery research, yet their evolution has followed a path of incremental advances rather than radical transformations. Their journey began in the 1960s with the development of *liposomes*, which were initially designed to encapsulate hydrophobic drugs, thereby improving solubility and reducing toxicity [13]. These early formulations, while groundbreaking, faced several limitations, including rapid clearance by the mononuclear phagocyte system (MPS) and instability in biological environments [14].

To address these shortcomings, the 1980s and 1990s saw the emergence of *PEGylated*

liposomes, with surface modifications designed to prolong circulation time and evade immune detection. A key milestone was the approval of *Doxil*, a PEGylated liposomal formulation of doxorubicin, which revolutionized cancer therapy by enhancing drug bioavailability and reducing systemic toxicity [15]. This marked the first major clinical success for lipid vesicles, solidifying their potential as versatile carriers.

Despite these advancements, challenges such as limited cargo versatility, non-specific uptake, and inefficient intracellular delivery persisted. Researchers explored targeted liposomes, functionalized with ligands or antibodies to improve specificity, as well as stimuli-responsive vesicles, engineered to release cargo in response to pH, temperature, or enzymatic triggers [17]. While these approaches introduced a level of precision, they did not fundamentally address the structural limitations of symmetric lipid vesicles, which rely on uniform bilayer compositions.

Only in recent years has interest shifted toward asymmetric lipid vesicles as described in the section above. Despite their promise, research on asymmetric lipid vesicles remains in its infancy. Questions surrounding uptake, physical characteristics and controlled fabrication techniques remain largely unanswered.

1.2.3 Challenges and Unknowns

As stated above, research on bi-layer asymmetric lipid vesicles is still in its early stages, and for all of their promise with packaging molecules of broad sizes and charges, there are multiple gaps in our knowledge about how these vesicles work. To reach a point where said vesicles can transport large, complex molecules such as proteins to target cells in patients who need them, we must understand these unknowns and optimize key characteristics to a level adequate for drug delivery systems.

Cellular Uptake and Endosomal Escape

Lipid vesicles primarily enter cells via **endocytosis**, a process in which the plasma membrane engulfs extracellular particles into vesicles. Several endocytic pathways contribute to lipid vesicle uptake, including *clathrin-mediated endocytosis*, *caveolae-mediated endocytosis*, *macropinocytosis*, and *phagocytosis* [13]. The choice of uptake mechanism depends on vesicle size, surface charge, and cell type.

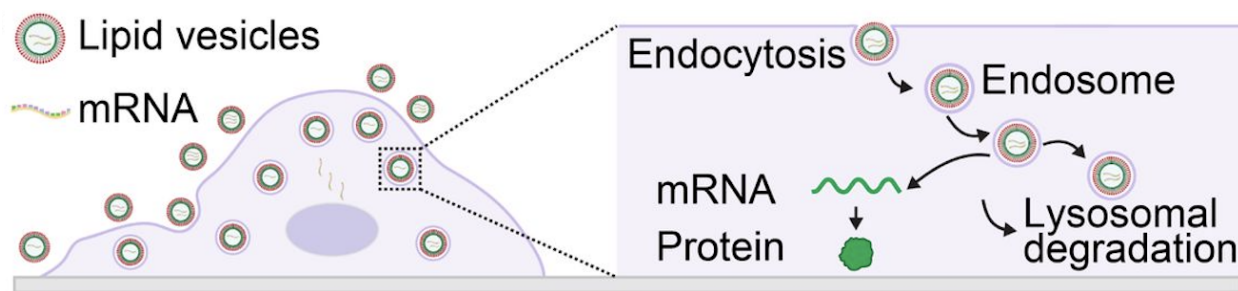


Figure 1.2: Endocytosis – Uptake Methodology of Vesicles by Cells

The foremost challenge in lipid vesicle-based drug delivery is that a significant portion of vesicles fail to be internalized by cells altogether, relative to existing drug delivery vehicles like those described above. This inefficiency reduces therapeutic efficacy, particularly for nucleic acid and protein-based drugs that require high intracellular concentrations to exert their effects.

Another major limitation of endocytosis-based uptake is that internalized lipid vesicles often become trapped inside **endosomes**, which later fuse with lysosomes. This results in acidic degradation of the vesicle, preventing the drug cargo from reaching its target site [17]. This is particularly problematic for nucleic acid therapies (e.g., mRNA, siRNA, and CRISPR), which require direct cytosolic access to be functional.

Cellular Uptake Factors

The uptake efficiency of lipid vesicles is influenced by multiple physicochemical parameters, including:

- **Zeta Potential:** Surface charge affects interactions with the cell membrane. Highly anionic vesicles often experience repulsion from the negatively charged cell surface, while cationic vesicles may exhibit strong adhesion but risk cytotoxicity [17].
- **Membrane Fluidity:** The rigidity or fluidity of the vesicle bilayer determines how vesicles interact with lipid rafts and endocytic machinery. More rigid vesicles may resist deformation, hindering endocytosis, whereas highly fluid vesicles may fuse too easily and lose structural integrity [16].
- **Bending Energy and Vesicle Geometry:** The curvature of the vesicle bilayer plays a key role in uptake, as cells preferentially internalize vesicles with certain geometric properties. While spherical vesicles are widely used, recent studies suggest that asymmetric or non-spherical vesicles may exhibit enhanced interactions with cellular membranes [15].

Encapsulation of Large Biomolecules

Encapsulation of large biomolecules, such as proteins and *CRISPR-Cas9* complexes, has been a longstanding challenge in lipid vesicle design [10]. While studies have shown that proteins can be successfully encapsulated within lipid vesicles, there is still work to be done in achieving high encapsulation efficiency while maintaining vesicle stability [11].

Stability and Scalability

Lipid vesicles must be stable in physiological conditions to prevent premature drug release. Factors such as lipid composition, vesicle size, and surface modifications play a critical role

in stability [12]. Additionally, scalable production methods are needed to translate lipid vesicle-based formulations from the lab to clinical applications [13].

1.2.4 Thesis Goals

We have covered the current landscape of drug delivery systems and recounted the constraints that all current systems face. We have hence established the need for a drug delivery vehicle that is not restricted by constraints of package size or charge, and have discussed the potential for lipid vesicles to circumvent these challenges, and to transport cutting-edge developments like the *CRISPR-Cas9* protein, among other gene editing proteins and complex drugs, to the body to achieve outcomes never before perceived as possible.

However, as discussed in the previous section, the most significant challenge currently hindering the development of lipid vesicles for drug delivery purposes is their limited uptake by cells.

This thesis then aims to explore this question of cellular uptake of lipid vesicles. To this end, we analyze the design of these lipid vesicles, and the role of vesicle symmetry, geometry, and lipid composition, on the uptake of said vesicles by human cells. Our specific goals are:

Specific Goals

- To apply differential geometry principles to understand vesicle shape and geometry in the context of endocytosis, and to evaluate how vesicle geometry influences cellular internalization.
- To investigate how lipid asymmetry affects cellular uptake efficiency. We aim to determine whether bilayer asymmetry (i.e., distinct inner vs. outer leaflet compositions) significantly enhances (or inhibits) uptake relative to symmetric vesicles.
- To understand the role of surface charge (zeta potential) and membrane fluidity on vesicle geometry and uptake efficiency.

- **To correlate geometric and biophysical vesicle parameters with the biological outcome of cellular uptake.** The aim is to identify optimal vesicle designs that maximize uptake while preserving payload stability and cellular viability (although payload stability and toxicity are outside the scope of this thesis).

By elucidating these factors, this study seeks to move one step closer to using lipid vesicles to expand the parameter space of cutting-edge, complex therapeutics that can be delivered to the human body to alleviate more disease than ever before.

1.2.5 Thesis Outline

Our goal with the next chapter is to establish the foundations of vesicle geometry and understand which parameters we can measure and tweak to optimize uptake. We hence start with a mathematical approach to understand and derive necessary equations and relationships between measurable quantities and established theories.

Next, we will give an overview of the methods and experiments conducted, noting the scientific underpinnings of said methods to explain why we made certain design choices, and to analyze each such choice under the lens of our research goal: to optimize vesicle uptake by cells.

Having detailed our methods, we will proceed to results, where we will share our findings on characterization studies and uptake quantification of multiple permutations of vesicles engineered and tested.

Lastly, we will move to a discussion about our findings, contextualizing them within our hypotheses and existing literature, and proposing future steps.

Chapter 2

Geometric and Symmetric Analysis of Lipid Vesicles

There is geometry in the humming of the strings, there is music in the spacing of the spheres.

PYTHAGORAS

2.1 Introduction

The study of lipid vesicle geometry provides crucial insight into the mechanics of cellular uptake. Biological membranes are inherently elastic structures whose physical behavior can be understood through the mathematical lens of differential geometry and variational calculus [20]. The curvature, symmetry, and elastic energy of these membranes are intimately connected to their interactions with the environment, particularly with the uptake pathways of target cells. In particular, vesicles undergo bending and tension during endocytosis, and their geometry-defined physical characteristics determine how easily they can be taken in through the uptake process described in the Introduction. In this chapter, we develop a rigorous geometric and symmetric analysis of lipid vesicles using the mathematical machinery of differential geometry, curvature tensors, and energy functionals. This foundation will inform the development of dynamical models and provide the tools necessary to interpret experimental data detailed in the next chapter.

Our first section begins by establishing the mathematical foundations of geometry which dictate vesicle structure, bending, curvature and tension, outlining established equations and applying them to our vesicles by contextualizing the different parameters and what they mean for our compartments. Having done this, the second section applies these concepts and integrates measurable quantities with the outlined equations, grounding our foundations in the sphere of drug delivery and particularly lipid vesicles.

2.2 Mathematical Foundations

2.2.1 Differential Geometry of Surfaces

We begin by modeling a lipid vesicle as a smooth, closed surface embedded in three-dimensional Euclidean space, \mathbb{R}^3 . Let S denote the surface of the vesicle, and suppose that S is parameterized by coordinates $(u, v) \in U \subset \mathbb{R}^2$ such that the embedding $\mathbf{X}(u, v) : U \rightarrow \mathbb{R}^3$ defines the shape of the vesicle.

To describe the geometry of the surface, we first define its tangent vectors. The partial derivatives of the embedding function $\mathbf{X}(u, v)$ with respect to u and v are tangent to the surface:

$$\mathbf{X}_u = \frac{\partial \mathbf{X}}{\partial u}, \quad \mathbf{X}_v = \frac{\partial \mathbf{X}}{\partial v}. \quad (2.1)$$

These vectors span the tangent plane at each point and are used to construct the first fundamental form, which encodes information about lengths and angles intrinsic to the surface.

The first fundamental form is a quadratic form on the tangent space, and is given by:

$$I = E du^2 + 2F du dv + G dv^2, \quad (2.2)$$

where the coefficients are defined by the inner products:

$$E = \mathbf{X}_u \cdot \mathbf{X}_u,$$

$$F = \mathbf{X}_u \cdot \mathbf{X}_v,$$

$$G = \mathbf{X}_v \cdot \mathbf{X}_v.$$

These expressions arise from the classical definition of a Riemannian metric induced by the immersion of a surface in \mathbb{R}^3 [21]. The fundamental form allows computation of lengths,

areas, and angles directly from the embedding.

Next, to study the curvature of the surface, we define the second fundamental form. This form encodes how the surface bends in space and is given by:

$$II = L du^2 + 2M du dv + N dv^2, \quad (2.3)$$

with coefficients:

$$L = \mathbf{X}_{uu} \cdot \mathbf{n},$$

$$M = \mathbf{X}_{uv} \cdot \mathbf{n},$$

$$N = \mathbf{X}_{vv} \cdot \mathbf{n},$$

where \mathbf{n} is the unit normal vector to the surface, defined (up to orientation) by:

$$\mathbf{n} = \frac{\mathbf{X}_u \times \mathbf{X}_v}{\|\mathbf{X}_u \times \mathbf{X}_v\|}. \quad (2.4)$$

These coefficients measure the normal components of the second derivatives of \mathbf{X} , and are interpreted geometrically as the directional curvatures of the surface in the directions of u and v .

The second fundamental form quantifies the extrinsic curvature of the surface—that is, how the surface is embedded in \mathbb{R}^3 . To further analyze this curvature, we introduce the shape operator S , a self-adjoint linear operator defined by:

$$S(\mathbf{v}) = -\nabla_{\mathbf{v}} \mathbf{n}, \quad (2.5)$$

where $\nabla_{\mathbf{v}} \mathbf{n}$ is the directional derivative of the normal vector in the direction of the tangent vector \mathbf{v} . The eigenvalues of S are the principal curvatures κ_1 and κ_2 .

Key Equation 1: Curvature

From these principal curvatures, we define two key scalar invariants of the surface:

$$H = \frac{\kappa_1 + \kappa_2}{2}, \quad K = \kappa_1 \kappa_2, \quad (2.6)$$

where H is the mean curvature and K is the Gaussian curvature.

Mean curvature quantifies the average bending of the surface, while Gaussian curvature reflects its intrinsic curvature, as it depends solely on the first fundamental form and not on the embedding. We will be employing these derived quantities, H and K , extensively for the rest of the chapter.

2.2.2 Helfrich Energy and Bending Rigidity

To quantify the energetic cost associated with deforming a lipid bilayer, we use the Helfrich bending energy model [22]. This model provides a phenomenological description of the curvature elasticity of lipid membranes and captures the key energetic contributions arising from membrane shape changes.

Key Equation 2: Bending Energy

The bending energy of a vesicle surface S is expressed as the functional:

$$F_{\text{bend}} = \int_S \left[\frac{\kappa}{2} (2H - C_0)^2 + \bar{\kappa}K \right], dA, \quad (2.7)$$

where:

- κ is the bending rigidity modulus, quantifying resistance to changes in mean curvature,
- H is the mean curvature of the surface,

- C_0 is the spontaneous curvature induced by asymmetry or external interactions,
- $\bar{\kappa}$ is the Gaussian rigidity modulus, related to topological changes,
- K is the Gaussian curvature,
- dA is the infinitesimal area element on the surface.

Derivation and Physical Interpretation of the Mean Curvature Term. The first term in the integrand, $\frac{\kappa}{2}(2H - C_0)^2$, penalizes deviation of the local mean curvature H from a preferred value $C_0/2$. The factor of 2 arises because the mean curvature H is defined as the average of the two principal curvatures, while the spontaneous curvature C_0 reflects a preferred total curvature.

The bending modulus κ typically ranges from 10 to 40, $k_B T$ for simple phospholipid membranes. A larger value of κ indicates that more energy is required to bend the membrane, reflecting higher mechanical stiffness.

If a membrane is symmetric and flat in its relaxed state, then $C_0 = 0$, and the energy is minimized when $H = 0$. For vesicles, this corresponds to shapes such as spheres of constant curvature or planar bilayers.

Origin and Role of the Spontaneous Curvature C_0 . Spontaneous curvature arises from asymmetries in the bilayer. For example, if the outer leaflet contains more lipids or bulky groups (e.g., PEG, cholesterol, proteins) than the inner leaflet, the bilayer prefers to bend in a specific direction. The constant C_0 models this preference mathematically.

Spontaneous curvature allows modeling of vesicles that bud, tubulate, or adopt non-spherical shapes. It is essential for capturing the diversity of shapes observed in biological membranes.

The Gaussian Curvature Term. The second term, $\bar{\kappa}K$, represents contributions from Gaussian curvature. By the Gauss-Bonnet theorem:

$$\int_S K dA = 2\pi\chi(S), \quad (2.8)$$

where $\chi(S)$ is the Euler characteristic of the surface (e.g., $\chi = 2$ for a sphere, $\chi = 0$ for a torus).¹ Because this integral is topologically invariant, this term contributes only when the topology changes—e.g., during vesicle fusion, fission, or pore formation.

The Gaussian modulus $\bar{\kappa}$ is often difficult to measure but empirically is of comparable magnitude (and often negative) relative to κ .

Total Energy and Variational Principles. The total bending energy can be minimized using calculus of variations. The Euler-Lagrange equation resulting from minimizing F_{bend} under a volume or area constraint leads to shape equations that predict equilibrium vesicle morphologies.

In the absence of constraints and with $C_0 = 0$, a sphere minimizes the energy, explaining why spherical vesicles are ubiquitous. If $C_0 \neq 0$, the equilibrium shape can deviate from a sphere, depending on the sign and magnitude of C_0 .

Biological Relevance. The Helfrich energy framework applies broadly to biological systems: red blood cell shapes, Golgi cisternae, membrane tubules, and synthetic vesicles. It provides a geometric basis for interpreting experimental observations and for predicting the behavior of vesicles under chemical and mechanical perturbations.

In later chapters, we will see how experimental measurements—such as bending modulus extracted via fluctuation spectroscopy or deformation under pipette suction—can be directly mapped onto the parameters κ and C_0 in this model. This geometric foundation serves as a

¹The Euler characteristic $\chi(S)$ is a topological invariant given by $\chi = V - E + F$ for a triangulated surface, where V , E , and F are the number of vertices, edges, and faces respectively. It provides a coarse measure of a surface's topology: for example, closed surfaces without holes have $\chi = 2$, while each added hole decreases the value by 2. For more details, see[21].

bridge between physical theory and experimental vesicle biology.

2.2.3 Membrane Tension and Area Expansion

Beyond bending, lipid bilayers can experience stretching due to osmotic pressure, binding interactions, or external mechanical forces. To capture the energetic cost associated with such deformations, we consider surface tension and area expansion energy, which are rooted in the theory of linear elasticity [23].

Key Equation 3: Tension

The surface tension σ is defined as the energy per unit increase in membrane area. When a membrane is stretched uniformly, the associated elastic energy per unit area can be modeled using Hookean elasticity:

$$F_{\text{tension}} = \frac{K_a}{2} \left(\frac{\Delta A}{A_0} \right)^2 A_0 = \frac{K_a}{2} \frac{(\Delta A)^2}{A_0}, \quad (2.9)$$

where:

- $\Delta A = A - A_0$ is the change in surface area,
- A_0 is the reference area of the vesicle (often taken as the equilibrium area),
- K_a is the area expansion modulus (units: energy per unit area).

This formulation arises from the definition of the linear strain $\varepsilon = \Delta A/A_0$. The quadratic form penalizes deviations from equilibrium, similar to a stretched elastic spring, and assumes that the stress is linearly proportional to the strain—a valid assumption for small deformations.

Interpretation of K_a . The area expansion modulus quantifies the membrane's resistance to in-plane stretching. Physically, K_a is determined by the strength of lipid-lipid interac-

tions and the degree of lipid packing. Higher values imply a tighter, more rigid structure, whereas low values suggest a more flexible, fluid membrane. Typical values for phospholipid membranes are on the order of 200–300 mN/m.

In the context of cellular uptake, changes in vesicle tension affect both stability and fusion capabilities. A higher tension typically corresponds to a greater tendency for vesicle rupture or permeabilization, whereas membranes under low tension can undergo invagination and internalization more readily.

For non-uniform strain, one generalizes the energy functional using a local surface strain field $\varepsilon(u, v)$:

$$F_{\text{tension}} = \frac{1}{2} \int_S K_a \varepsilon^2(u, v), dA, \quad (2.10)$$

where the strain $\varepsilon(u, v)$ is computed from the change in the first fundamental form of the surface.

This geometric reinterpretation of in-plane stretching allows us to connect classical elasticity theory with differential geometry, which becomes crucial for modeling mechanically deformed or tethered vesicles.

2.2.4 Spontaneous Curvature and Asymmetry

The lipid composition of vesicles often exhibits asymmetry between the inner and outer leaflets. This asymmetry can arise naturally during vesicle formation or be engineered via the insertion of polymers, cholesterol, or proteins into only one leaflet. Such asymmetry creates a preferred direction of curvature, known as spontaneous curvature [24].

Key Equation 4: Spontaneous Curvature

Mathematically, we model this by introducing a spontaneous curvature constant C_0 into the Helfrich energy:

$$F_{\text{bend}} = \int_S \frac{\kappa}{2} (2H - C_0)^2, dA. \quad (2.11)$$

To understand its effect, suppose the vesicle is spherical with radius R . For a sphere, the mean curvature $H = 1/R$. Substituting this into the energy functional yields:

$$F_{\text{bend}}(R) = 2\pi\kappa \left(1 - \frac{R}{R_0}\right)^2, \quad (2.12)$$

where $R_0 = 1/C_0$ is the preferred radius of curvature.

The energy is minimized when $R = R_0$, confirming that the vesicle tends to adopt a radius compatible with its asymmetry.

Biophysical origin of C_0 . The spontaneous curvature reflects the imbalance of forces between the two leaflets. For instance, if the outer leaflet contains larger headgroup lipids, it tends to expand more than the inner leaflet, causing the vesicle to bend inward. Conversely, if cholesterol or PEG is inserted asymmetrically, C_0 may favor outward curvature.

Thermodynamically, this asymmetry may be driven by differences in entropy, lipid-lipid interactions, or curvature-inducing proteins. Experimentally, C_0 can be inferred by analyzing vesicle morphologies or by manipulating leaflet asymmetry through chemical treatments. Control of C_0 enables the engineering of vesicles for targeted delivery, as vesicles with optimal curvature may show enhanced fusion or uptake.

This spontaneous curvature model plays a crucial role in connecting geometry to cellular behavior and will underpin future discussions on uptake mechanisms.

2.3 Measurable Geometric Properties and Theoretical Interpretation

To relate our mathematical models to experimental practice, we identify physical quantities that can be measured and interpreted through geometric theory.

2.3.1 Membrane Fluidity and Laurdan GP

Membrane fluidity reflects the lateral mobility of lipid molecules and is influenced by lipid packing, phase state, and curvature. Laurdan (6-dodecanoyl-2-dimethylaminonaphthalene) is a membrane dye whose fluorescence spectrum depends on lipid order.

The Generalized Polarization (GP) is calculated as:

$$\text{GP} = \frac{I_{440} - I_{490}}{I_{440} + I_{490}}, \quad (2.13)$$

where I_{440} and I_{490} are fluorescence intensities at 440 nm and 490 nm, respectively. A high GP value indicates ordered (gel-like) membranes, while low GP suggests disordered (fluid-like) membranes.

From a geometric standpoint, fluid membranes more readily adopt deformed configurations. A correlation often exists between GP and bending rigidity κ , with more fluid membranes typically having lower κ , thus enabling greater curvature and uptake [25]. This inverse relationship has been observed in experimental systems [26] and can be modeled by a phenomenological equation:

Key Equation 5: GP and κ

$$\kappa = \kappa_{\max} - \lambda \cdot (1 - \text{GP}), \quad (2.14)$$

where κ_{\max} is the bending rigidity in the gel phase (high order), λ is a material-dependent

proportionality constant, and $1 - GP$ reflects the degree of fluidization.

This expression provides a quantitative route for estimating curvature elasticity based on fluorescence measurements of lipid order.

2.3.2 Surface Charge and Zeta Potential

The zeta potential ζ is a measure of the surface electrostatic potential at the slipping plane of a vesicle in solution. It influences vesicle-vesicle and vesicle-cell interactions by affecting the electric double layer surrounding the vesicle, which can modulate both adhesion and repulsion forces in biological media.

Mathematically, ζ does not explicitly enter the original Helfrich model, which is curvature-based and electrostatically agnostic. However, an important extension—and one of the efforts of this thesis—is to consider how electrostatics, as captured by ζ , can modulate the effective bending rigidity κ through changes in lipid packing and osmotic pressure gradients.

Specifically, membranes with high surface charge (either positive or negative) exhibit increased electrostatic repulsion between adjacent lipid headgroups. This repulsion can lead to a local expansion of the membrane, decreasing lipid packing density and increasing membrane fluidity. In such cases, we hypothesize and will explore experimentally whether:

$$\kappa_{\text{eff}} = \kappa_0 - \gamma|\zeta|, \quad (2.15)$$

where κ_{eff} is the effective bending rigidity, κ_0 is the intrinsic bending rigidity in the absence of electrostatic contributions, and γ is a proportionality constant to be empirically determined from our experimental data.

Zeta potential is measured via electrophoretic mobility and provides insights into the net surface charge distribution. This becomes particularly relevant in the engineering of vesicles for drug delivery, where high ζ values (typically from cationic lipids or charged polymers)

can promote electrostatic adhesion to negatively charged cell membranes, enhancing uptake.

2.3.3 Micropipette Aspiration and Bending Modulus

Micropipette aspiration experiments stretch vesicles by applying suction through a narrow pipette [27]. From the deformation response, one extracts mechanical moduli.

Let ΔP be the suction pressure, R_p the pipette radius, R_0 the vesicle radius, and ΔL the aspirated tongue length. The surface tension is given by:

$$\sigma = \frac{R_p \Delta P}{2(1 - R_p/R_0)}. \quad (2.16)$$

The relative area change is approximated by:

$$\frac{\Delta A}{A_0} = \frac{\Delta L}{R_p}. \quad (2.17)$$

Plotting σ vs. $\Delta A/A_0$ yields the slope K_s , the stretching modulus:

$$K_s = \frac{d\sigma}{d(\Delta A/A_0)}. \quad (2.18)$$

Key Equation 6: Bending Modulus κ

To extract the bending modulus κ , one can analyze the thermal fluctuations of vesicle contours or apply small deformations and use the relation:

$$\kappa = \frac{k_B T}{8\pi} \left(\frac{\langle h^2 \rangle}{R^2} \right)^{-1}, \quad (2.19)$$

where $\langle h^2 \rangle$ is the mean square height fluctuation and R is the vesicle radius.

These techniques provide direct connections between experimental observations and geometric theory, enabling rigorous interpretation of vesicle mechanics.

2.4 Perspective

In this chapter, we have developed a mathematically rigorous framework for the geometric and symmetric analysis of lipid vesicles. By grounding the analysis in differential geometry and elasticity theory, we provide the theoretical foundation necessary to interpret biophysical measurements such as Laurdan GP, zeta potential, and micropipette aspiration. These models allow us to make sense of curvature-induced phenomena and asymmetry-driven uptake mechanisms, laying the groundwork for quantitative models in subsequent chapters.

Chapter 3

Designing and Testing the Lipid Vesicle – Methods

This chapter recounts the methodology used to design, fabricate, and characterize the lipid vesicles discussed in this thesis. We note key takeaways and pointers on parts of the design process which are integral to the eventual performance and uptake of these vesicles by grounding them in scientific theory and our knowledge of lipids and endocytosis. To learn more about specific experiment conditions, please refer to the Experimental Section in the Appendix.

The first section of this chapter will focus on the fabrication of the vesicle, detailing its structure, engineering methodology, and the different permutations of lipid composition tested for the vesicles. The second section will focus on the characterization and performance tests conducted on the engineered vesicles, including uptake measurements in HEP G2 liver cells, as well as the characterization measurements proposed in the previous chapter.

3.1 Designing the Vesicle

3.1.1 Bi-leaflet Lipid Vesicles

The vesicles engineered in this thesis were designed to mimic biological membranes by implementing **asymmetric bilayers**—wherein the inner and outer leaflets are composed of different lipid species. Biological plasma membranes are inherently asymmetric, with lipid composition differing across leaflets, which has implications for curvature, rigidity, and membrane interaction with cellular components [24]. By mimicking this asymmetry, we seek to better model biological behavior and optimize vesicle uptake by target cells.

As controls, **symmetric vesicles** were also constructed, in which both leaflets shared the same lipid composition. This provided a reference against which to measure the effects of asymmetry on vesicle stability, fluidity, surface charge, and uptake efficiency.

3.1.2 Lipid Composition Permutations

To investigate the effects of membrane asymmetry, surface charge, and lipid structure on vesicle uptake and performance, we systematically varied the lipid used in the outer leaflet of our bi-layered vesicles. A total of twelve lipids were selected, grouped into three categories based on their net charge at physiological pH: cationic, anionic (negatively charged), and zwitterionic (neutral).

For each lipid X in the outer leaflet, we constructed two vesicle types:

1. **Asymmetric vesicles:** outer leaflet = [Lipid X]; inner leaflet = POPC
2. **Symmetric vesicles:** both inner and outer leaflets = [Lipid X]

Just as a note for vesicle naming throughout this thesis, we always refer to vesicles as their *Inner Leaflet / Outer Leaflet* compositions. For example, in the example below, the

image on the right has POPC as its inner leaflet, and EPC as its outer leaflet, and so we would refer to it as a *POPC/EPC* vesicle.

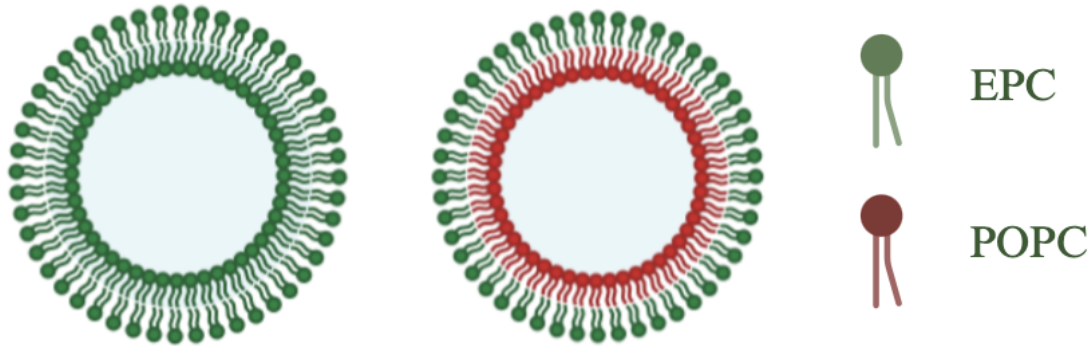


Figure 3.1: Asymmetric and Symmetric Nanoscale Lipid Vesicles

The list of tested lipids and their classification is provided in Table 3.1.

Table 3.1: Classification of lipids used for vesicle compositions

Cationic (Positive)	Anionic (Negative)	Neutral (Zwitterionic)
EPC	POPS	POPC
DLin-MC3	DOPS	DOPC
DOBAQ	DOPG	DOPE
DOSPA	POPG	POPE

Choosing POPC as the Inner Leaflet

In all asymmetric vesicle designs, the inner leaflet lipid was fixed as **1-palmitoyl-2-oleyl-sn-glycero-3-phosphocholine** (POPC), a zwitterionic phosphatidylcholine. This choice was made for several interrelated biochemical and biophysical reasons:

Rationale for Choosing POPC

- 1. Biological Relevance:** POPC is a major component of eukaryotic plasma membranes and is especially abundant in the inner cytoplasmic leaflet of mammalian cells. Its prevalence in natural membranes makes it an ideal baseline for modeling intracellular interactions [28].
- 2. Zwitterionic Nature:** POPC carries no net charge at physiological pH, which prevents strong electrostatic interactions with either cationic or anionic drug payloads. This neutrality helps ensure that encapsulated cargo does not experience significant membrane-associated perturbation during fabrication or storage [29].
- 3. Membrane Fluidity and Phase Behavior:** POPC remains in the fluid phase at room and physiological temperatures ($T_m \approx -2^\circ\text{C}$). This ensures that the inner leaflet retains lateral fluidity during vesicle fabrication, minimizing leaflet-specific lipid packing defects that could compromise bilayer integrity or permeability [30].
- 4. Structural Symmetry and Packing:** The cylindrical geometry of POPC molecules (headgroup area \approx tail area) supports a flat, bilayer-favoring structure. This contrasts with cone-shaped lipids like DOPE or POPE, which introduce spontaneous curvature. By maintaining POPC in the inner leaflet, we avoid confounding curvature effects when studying the influence of outer leaflet composition alone [31].
- 5. Encapsulation Stability:** The stability of the aqueous core in inverted vesicle fabrication is strongly influenced by the inner leaflet lipid. POPC, due to its neutral charge and well-packed bilayer structure, provides a stable encapsulating interface for a broad range of payloads, including proteins, RNAs, and dyes [32].

Thus, the use of POPC as a fixed inner leaflet provided a biophysically consistent and experimentally stable scaffold against which the effects of outer leaflet lipids (varying in charge, curvature, and fluidity) could be systematically interrogated.

3.1.3 Vesicle Engineering Technique

The vesicles were fabricated using a modified inverted emulsion technique followed by a precise extrusion protocol. This process enables the production of monodisperse, bi-leaflet vesicles of controlled lipid composition.

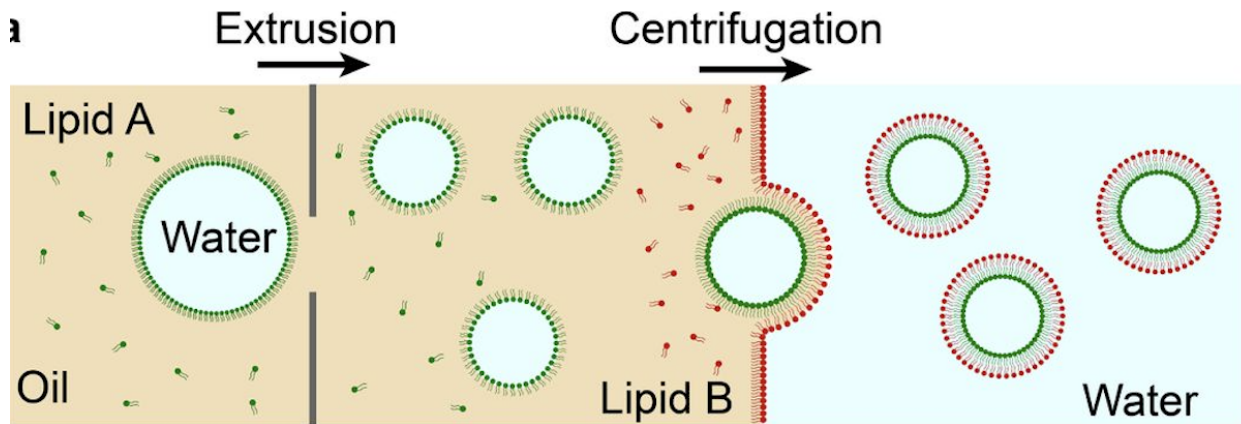


Figure 3.2: Engineering Method of Lipid Vesicles

The inverted emulsion method relies on forming a water-in-oil emulsion in which the inner aqueous droplets are surrounded by a monolayer of lipids. This water-in-oil emulsion is then passed through a membrane with pores of a set size, and extrusion is done at least 7 times back and forth between the membrane to ensure high yield. Upon centrifugation through a second monolayer at the oil-water interface, a second lipid leaflet is acquired, forming a bilayer vesicle [33]. By controlling the lipid compositions of each monolayer, one can fabricate asymmetric vesicles.

Extrusion through porous membranes ensures uniform vesicle size distribution, and this monodispersity is critical for reproducible biophysical characterization [32]. For the purposes of this thesis, we engineered and tested vesicles with a size of 200 nm, as these are around the sizes that would be employed for actual drug delivery vehicles and can permeate into cells given optimal uptake conditions.

3.2 Testing Vesicle Performance and Characteristics

3.2.1 Membrane Fluidity

Plate Reader Measurements Using Laurdan Dye

Membrane fluidity was assessed using the polarity-sensitive dye Laurdan (6-dodecanoyl-2-dimethylaminonaphthalene), which integrates into the vesicle bilayer and exhibits a spectral shift based on lipid packing. More ordered (gel-like) membranes result in a blue shift in emission (440 nm), while disordered (fluid-like) membranes emit more at 490 nm [34].

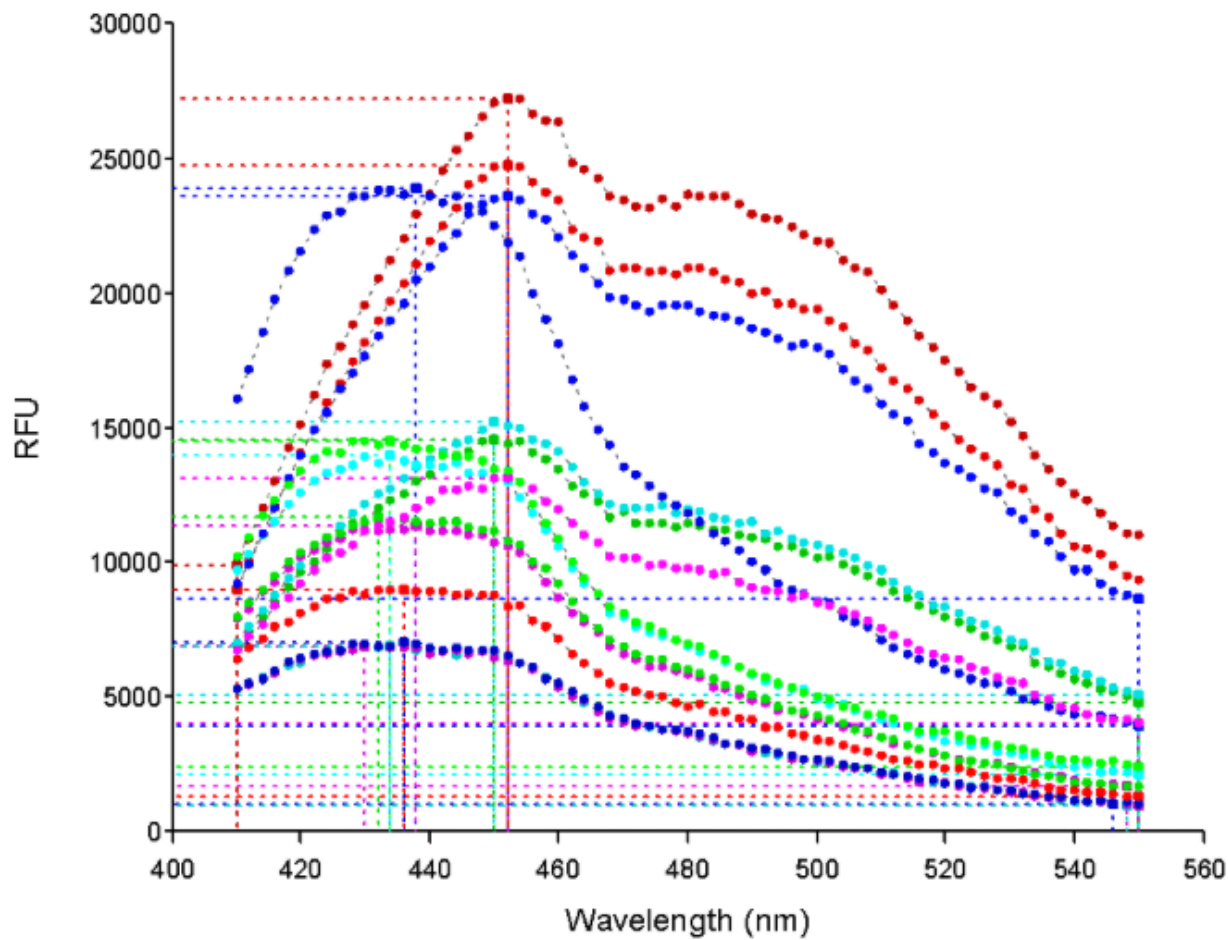


Figure 3.3: Emission Shifts of Vesicles Using Laurdan

Vesicles were labeled with Laurdan at a 1:200 molar ratio relative to total lipid during

fabrication. A volume of 100 μL of vesicle solution was transferred to a 96-well black clear-bottom plate. Emission spectra from 400 to 550 nm were collected with excitation at 350 nm. Each condition was measured in triplicate wells to account for variability and permit statistical averaging.

GP Calculation Pipeline

Data processing was performed using a custom Python analysis suite. The steps were as follows:

1. **Control Subtraction:** Background fluorescence from blank wells (no dye or lipid) was subtracted from experimental wells using the ‘`folder_subtract_control()`’ function.
2. **Spectral Normalization:** Emission values were normalized to local maxima to correct for variations in overall intensity using ‘`folder_norm()`’.
3. **Peak Extraction and Curve Fitting:** Fluorescence intensities at 440 nm and 490 nm were extracted using two methods:
 - Direct intensity comparison at 440 nm and 490 nm.
 - Fitting the emission curve using a sum of two Lorentzian functions centered at 440 and 490 nm respectively, yielding amplitudes A_{440} and A_{490} .
4. **GP Computation:** The Generalized Polarization (GP) value was computed for each replicate using:

$$\text{GP} = \frac{I_{440} - I_{490}}{I_{440} + I_{490}},$$

where I_{440} and I_{490} were either directly extracted intensities or Lorentzian amplitudes.

5. **Statistical Aggregation:** The mean and standard deviation of GP values were reported across triplicates for each condition.

This automated workflow allowed for high-throughput, reproducible quantification of membrane order, which was then used to infer relative fluidity among the 24 vesicle formulations tested. A higher GP value indicates a more ordered, rigid membrane, whereas lower values signify increased fluidity and lateral lipid diffusion.

3.2.2 Zeta Potential for Chemical Asymmetry

The surface electrostatic potential (zeta potential, ζ) of each vesicle formulation was measured using electrophoretic light scattering via a Zetasizer Dynamic Light Scattering instrument. The vesicle samples were diluted in 1 mL of Milli-Q water, and then folded capillary cells at room temperature were used to measure the zeta potential, again averaging out triplicates of values for consistency and precision.

Zeta potential reflects the surface charge of the outer leaflet and plays a role in colloidal stability, vesicle-cell interactions, and uptake efficiency.

We further proposed a curvature-modifying role for ζ , hypothesizing that surface charge could reduce the effective bending rigidity via:

$$\kappa_{\text{eff}} = \kappa_0 - \gamma|\zeta|, \quad (3.1)$$

where γ is a proportionality constant determined empirically.

3.2.3 Uptake Measurement

For the dependent variable in all our experiments and the parameter that this thesis aims to maximize – cell uptake – we used human HEP G2 liver cells to measure uptake of our fabricated vesicles, dyed with *Rhodamine – PE* dye for fluorescence and containing an ‘empty’ package of aqueous solution.

Vesicle uptake by human cells was quantified using two orthogonal techniques—confocal microscopy for spatial confirmation and flow cytometry for high-throughput quantification.

HEP G2 Cells for Uptake Measurement

All cellular uptake assays in this study were conducted using the HEP G2 cell line, a well-established human hepatocellular carcinoma cell model. This choice was made based on both pharmacological and physiological considerations relevant to lipid vesicle-based drug delivery.

Rationale for Choosing HEP H2 Cells)

1. Biological Rationale: Liver as the First Barrier: In vivo, intravenously administered nanoparticles, including lipid vesicles, invariably pass through the liver—the body’s central metabolic and detoxification organ—before reaching their final destination. The liver is perfused by both the hepatic artery and the portal vein, acting as a filtration and clearance interface for all substances entering systemic circulation. Therefore, *the liver is often the first biological checkpoint encountered by synthetic vesicles in the bloodstream* [12]. HEP G2 cells serve as an effective in vitro proxy for hepatocyte interaction, allowing us to evaluate how our vesicles might behave upon first contact with human liver tissue.

2. Lack of Targeting Ligands and Liver Predominance: In this study, vesicles were not functionalized with targeting moieties such as galactose-based ligands (for hepatocytes), polysaccharides (for macrophages), or folate (for tumor cells). In the absence of such modifications, vesicle distribution upon systemic administration is primarily governed by physicochemical properties—size, surface charge, and fluidity. Given that the liver has high nanoparticle uptake capacity, especially via Kupffer cells and sinusoidal endothelial cells, the HEP G2 line was an appropriate initial model to evaluate **non-targeted uptake pathways** [35].

3. Relevance to Drug Delivery Research: HEP G2 cells are commonly used in nanomedicine and pharmacokinetics research due to their:

- Human origin and hepatocyte-like metabolic enzyme expression;

- Polarized epithelial morphology and well-differentiated status;
- Ability to form tight junctions and simulate aspects of the hepatic barrier;
- Predictive power for hepatocellular uptake, metabolism, and drug-induced toxicity [36].

These attributes allow for the quantitative and qualitative evaluation of nanoparticle-cell interactions, including endocytic uptake, lysosomal trafficking, and membrane fusion dynamics. In our context, they served as a robust platform for evaluating the role of membrane fluidity, curvature, and surface charge on vesicle internalization.

4. Liver-Specific Considerations: The liver's dual role as both a metabolic hub and a clearance organ imposes unique challenges for drug delivery vehicles. Nanoparticles must avoid excessive liver clearance to reach peripheral tissues, but may also be designed for *intentional* liver targeting, especially for diseases like hepatocellular carcinoma or hepatitis B/C. Thus, understanding how vesicles interact with hepatic cells provides crucial insight into both potential off-target effects and therapeutic liver applications.

Moreover, the liver is rich in scavenger receptors and pattern recognition proteins that recognize surface features of nanoparticles—especially those with extreme zeta potentials or exposed phosphatidylserine—underscoring the importance of vesicle surface characteristics, which we varied systematically in this study.

This cell line, therefore, provided a biologically grounded and experimentally tractable model for screening the performance of engineered lipid vesicles in drug delivery contexts.

Confocal Microscopy

Confocal microscopy provided spatial resolution of vesicle internalization.

Vesicles were labeled with 1% Rhodamine-PE, while HEP G2 cells were seeded in 8-well

3.2 – Testing Vesicle Performance and Characteristics

chambers and incubated for 24 hours. The vesicles were then added at a concentration of 100 µg/mL and incubated for 4 hours. Cells were washed, fixed, and stained with DAPI before imaging on a Zeiss LSM900 Live Cell confocal microscope.

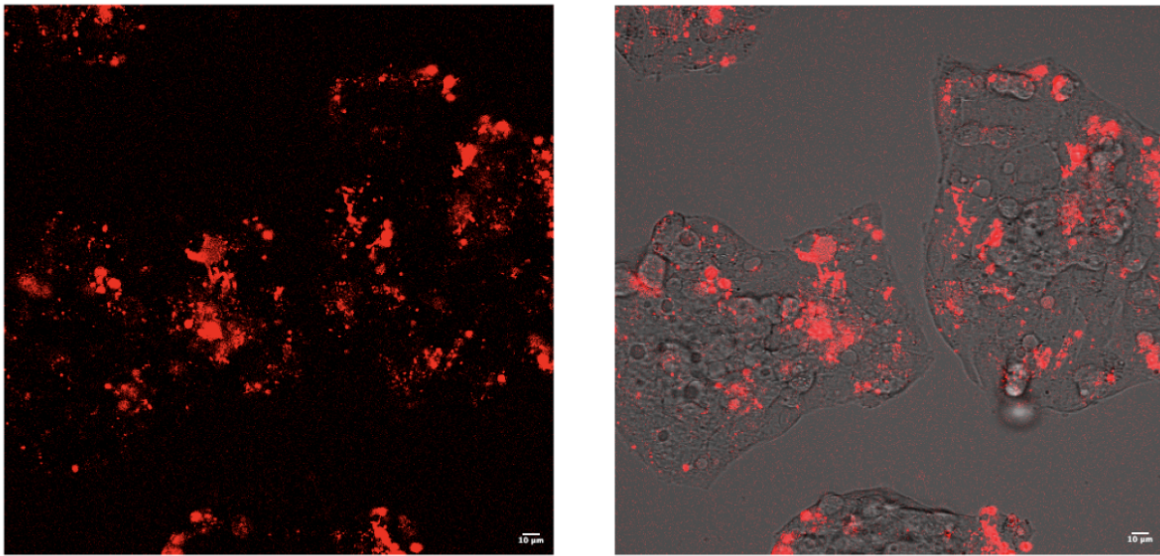


Figure 3.4: Example of Fluorescence Images Using POPC/EPC Vesicles. The left image shows just the fluorescence, while the right image shows the composite image of fluorescence and Brightfield imaging. The intensity of the red dye is correlated with the quantity of vesicles that were taken up by the cells being imaged.

Flow Cytometry

To quantify uptake across thousands of cells, we can employ flow cytometry.

For that goal, cells are incubated with rhodamine-labeled vesicles under identical conditions. 10,000 events per sample are recorded using a BD FACSaria instrument, and Mean fluorescence intensity (MFI) in the rhodamine channel is compared across conditions.

The resulting fluorescence intensities are normalized to the symmetric POPC/POPC vesicles as baseline.

Chapter 4

Results

This chapter presents the key experimental results of this study. The primary aim is to quantify and compare uptake efficiency of various lipid vesicle formulations using fluorescence intensity as a proxy, and then correlate these uptake levels with three central physical membrane properties: surface charge (zeta potential), and membrane fluidity (Laurdan GP), and the distinction between symmetric and asymmetric vesicles to assess how leaflet composition affects delivery potential.

Unlike Chapter 2, which focused on theoretical modeling, this chapter remains empirical and data-driven. The geometric and energetic interpretations of these results will be addressed in Chapter 5 (Discussion).

The main results presented are:

- Uptake differences between symmetric and asymmetric vesicles.
- The role of zeta potential in modulating uptake.
- The influence of membrane fluidity (GP) on uptake.
- A combined analysis of all three variables to identify dominant correlations.

4.1 Symmetric vs Asymmetric Vesicles

We first stratify vesicles into symmetric and asymmetric categories based on inner and outer leaflet composition. Symmetric vesicles have identical lipid compositions on both leaflets, whereas asymmetric vesicles contain distinct lipids on each side, engineered via inverted extrusion. For our research, the asymmetric vesicles kept the inner layer constant as *POPC*, for reasons detailed in Chapter 3.

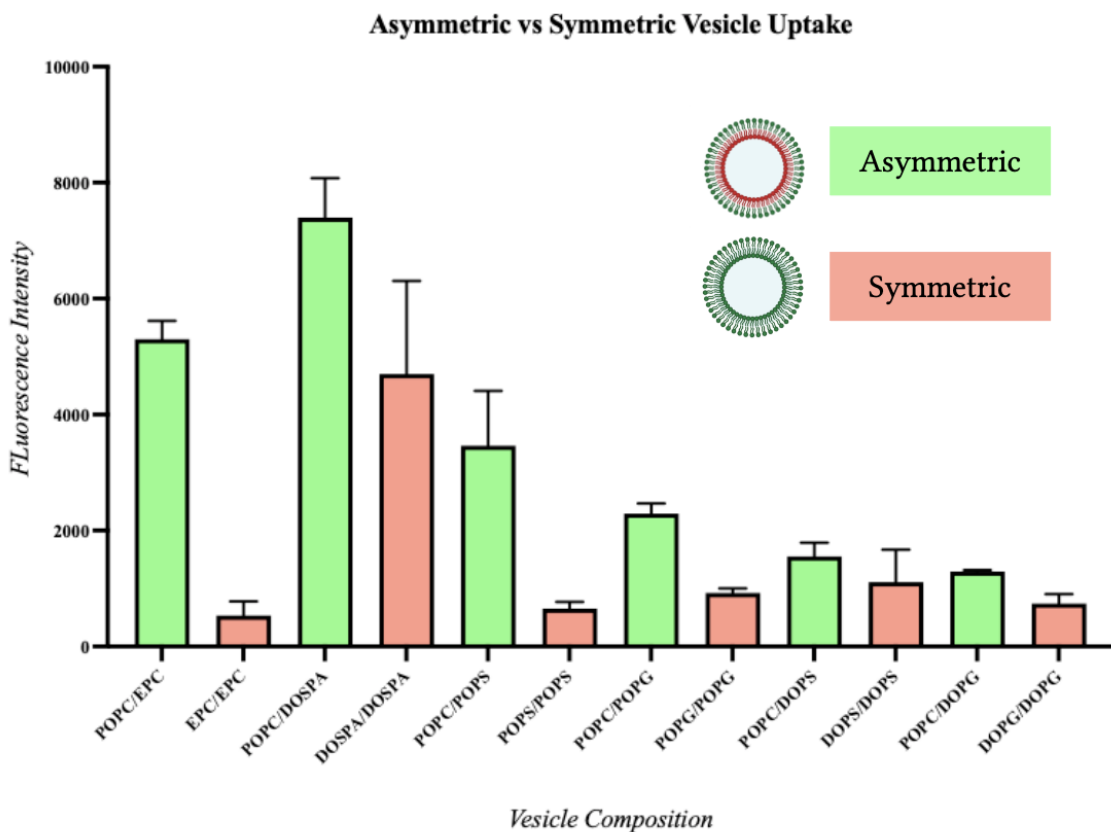


Figure 4.1: Uptake (Fluorescence Intensity) of Asymmetric and Symmetric Vesicles

As can be seen in Figure 4.1, for every single lipid chosen, the asymmetric version with an inner layer of *POPC* outperforms its symmetric counterpart (where both inner and outer layers are formed of the lipid chosen). The lipids not shown in this graph did not exhibit optimal uptake for either asymmetric or symmetric vesicles, but in those, there was a similar

multiple for the asymmetric fluorescence as opposed to the symmetric counterparts.

This confirms our thesis hypothesis that asymmetric lipid vesicles will exhibit greater uptake by cells owing to their likeness to similarly asymmetric cell membranes, as well as effects on vesicle geometry which will be discussed later.

We have also shown a visual example of the uptake of said vesicles in two particular lipid choices, one for a cationic and one for an anionic lipid, to show the extent of impact that asymmetry has on uptake.

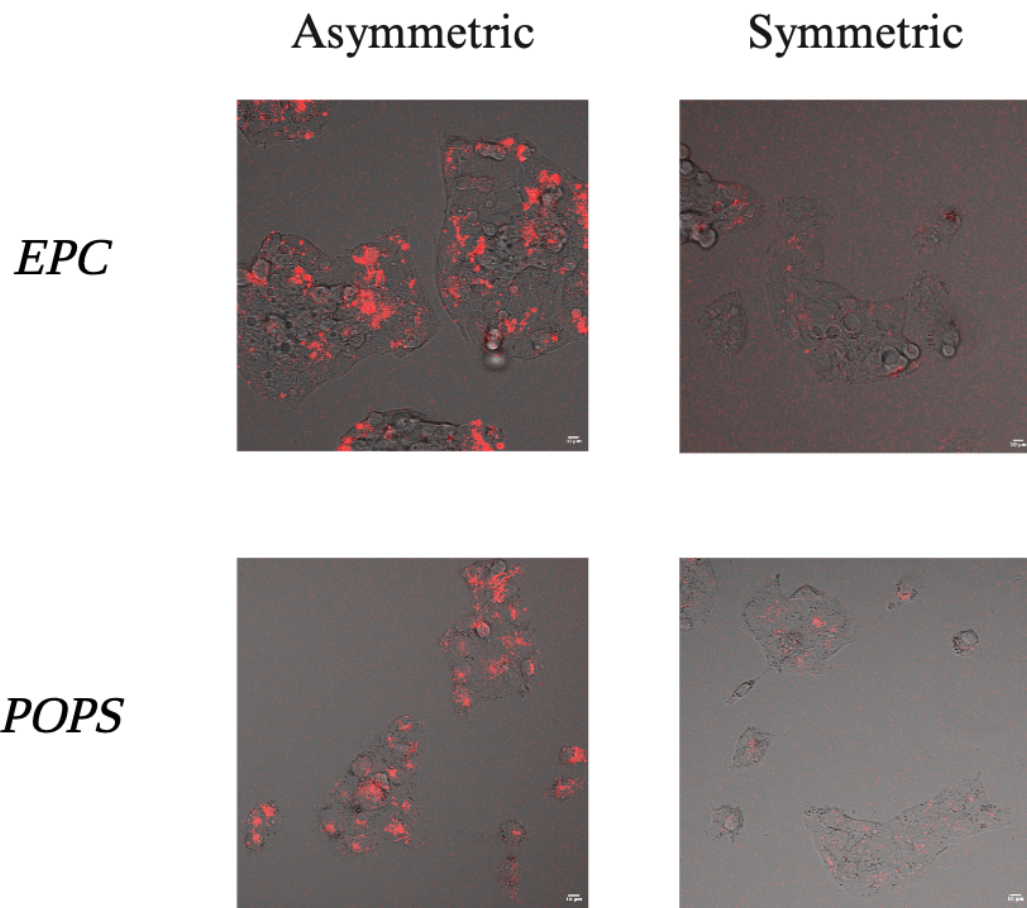


Figure 4.2: Asymmetric Vesicle Uptake Compared to Symmetric Counterparts for EPC (Cationic) and POPS (Anionic) Lipids.

4.2 Zeta Potential and Cellular Uptake

We next examine how vesicle surface charge, as measured by zeta potential, affects uptake levels. Zeta potential reflects the surface electrostatics of the lipid bilayer, which can influence vesicle interaction with negatively charged cell membranes.

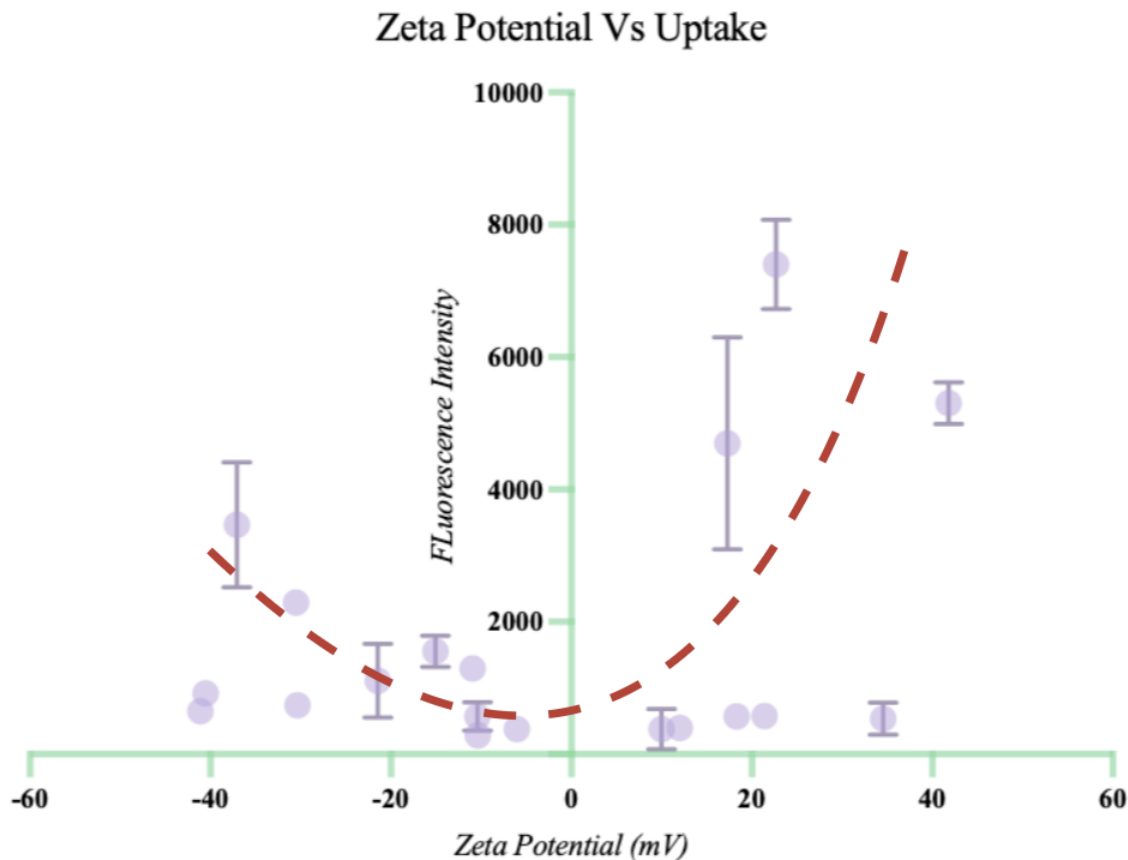


Figure 4.3: Scatterplot of Zeta Potential Values with Uptake (Measured through Fluorescence Intensity)

Figure 4.3 reveals a non-linear relationship between zeta potential and uptake. **Vesicles with strongly positive zeta potentials (+20 to +45 mV) exhibit the highest fluorescence intensity**, suggesting enhanced uptake likely mediated by electrostatic attraction to negatively charged cell membranes. We see, however, in the line of best fit,

that **there is an extreme-leaning tendency also – vesicles with strongly negative zeta potentials (-35 to -45 mV) also exhibit high uptake, whereas vesicles with near-neutral zeta potential (0 mV) show uniformly poor uptake.**

This pattern implies that it is not merely the sign of the surface charge, but the magnitude of the electrostatic potential that influences delivery efficiency. This feeds into our hypothesis in Chapter 2 that zeta potential not only affects uptake through electrostatic interactions with surroundings, but also by impacting the geometry and bending of the vesicle itself, thus indicating that higher charge (regardless of sign) impacts the vesicle and causes it to deform and be taken in through endocytosis with more ease.

4.3 Membrane Fluidity (GP) and Cellular Uptake

Membrane order was assessed using Laurdan GP (generalized polarization), which provides a readout of lipid packing and fluidity. Higher GP values indicate more ordered and hence less fluid membranes.

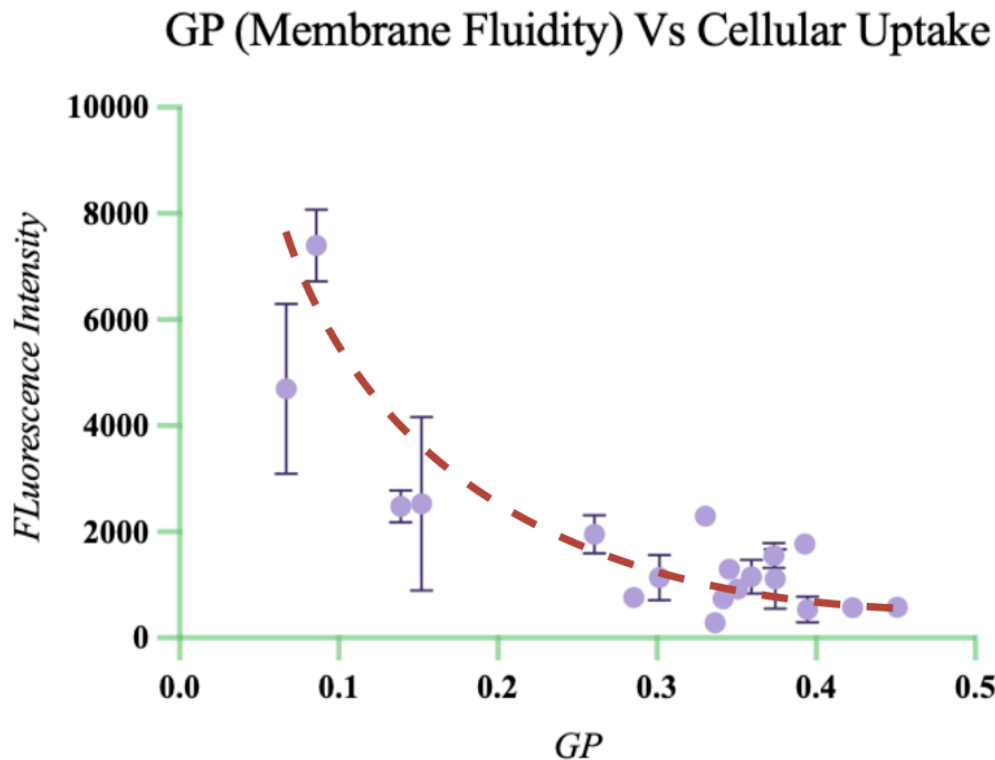


Figure 4.4: Scatterplot of Membrane Fluidity (GP) with Uptake

The trendline in the scatterplot above suggests that more fluid (disordered) membranes (which are indicated by lower GP values) enhance uptake – consistent with the hypothesis that flexible membranes deform more easily to wrap around or fuse with cellular membranes, as is required for successful endocytosis. It is also noteworthy that the relationship is not a linear one, although the sample size of 20 vesicles is perhaps not enough to empirically state that the relationship possesses a certain order or the other.

4.4 Multi-Parameter Correlation

To further emphasize the interdependence of uptake on zeta potential, GP, and asymmetry, we perform a multi-parameter analysis.

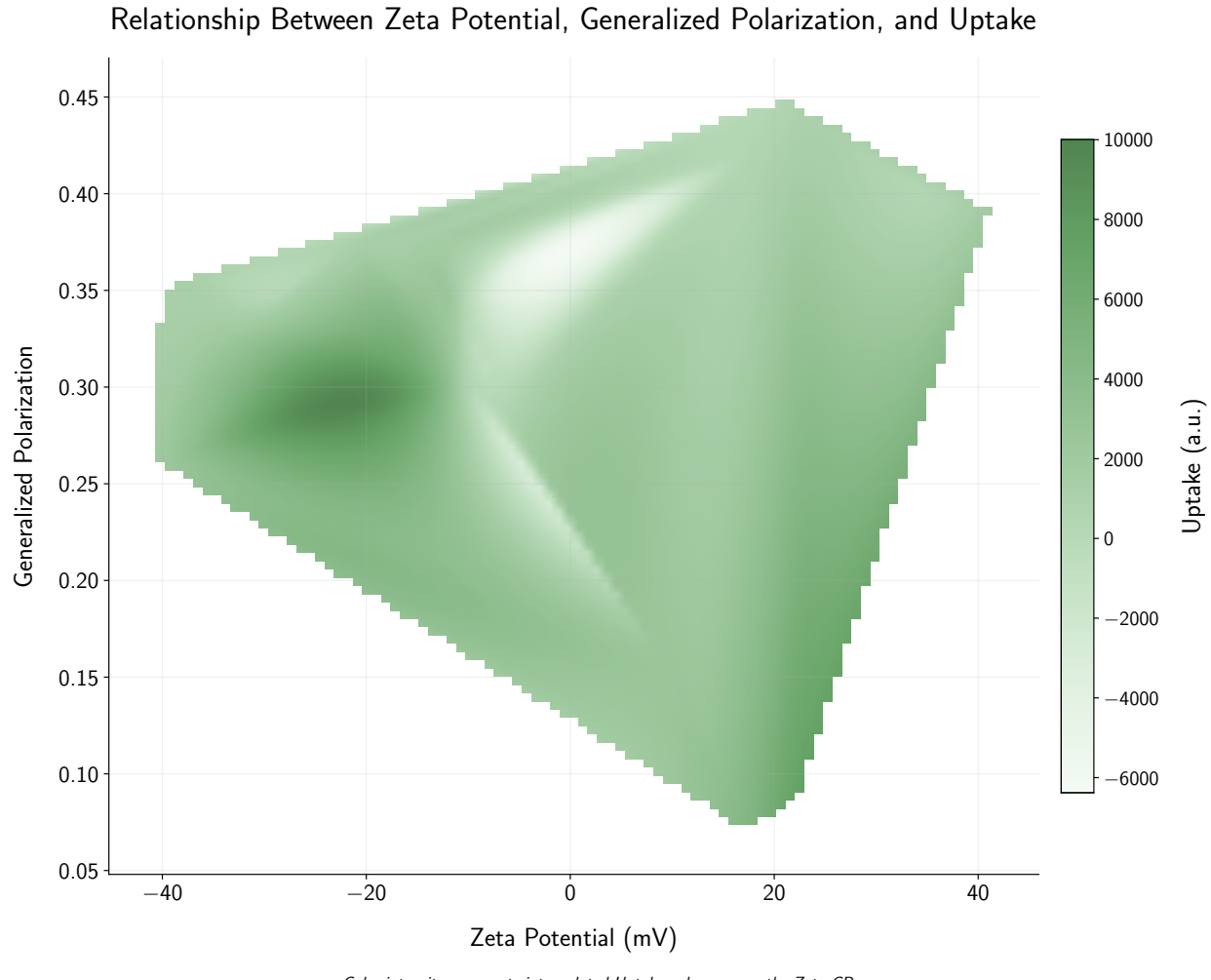


Figure 4.5: Heatmap visualization of the relationship between Zeta Potential (mV), Generalized Polarization, and Uptake. Color intensity represents interpolated Uptake values (a.u.) across the Zeta-GP parameter space, with greater intensity indicating higher Uptake. The continuous surface is generated using cubic interpolation of experimental data points spanning both positive and negative Zeta Potential ranges.

We observe that the darkest region of the graph occurs in the bottom right, which is where we have a high zeta potential and a low GP (which translates to high membrane fluidity).

4.5 Summary of Observations

Key Results Summary

- Asymmetric vesicles exhibit significantly higher uptake than their symmetric counterparts. This was exhibited by 10 of the 12 lipids tried, with the remaining 2 not exhibiting much uptake either way.
- Large positive ζ values exhibit the highest uptake, as they interact favorably with the negative cell membrane. In general, higher magnitude zeta potential values are taken up at a higher frequency than lower magnitude values closer to 0 mV. The relationship had tendencies toward the extrema.
- Membrane fluidity is inversely/directly related to uptake – more disordered, fluid membranes exhibited higher levels of fluorescence intensity and hence cellular uptake.

We will now place these findings within a theoretical framework, comparing experimental trends with predictions from membrane curvature models and differential geometry, and thus trying to explain cellular uptake from a theoretical perspective in addition to just an empirical one.

Chapter 5

Bridging the Empirical and the Theoretical – Discussion

This chapter synthesizes the empirical results from Chapter 4 with the mathematical and geometric models developed in Chapter 2. The aim is to provide a mechanistic understanding of lipid vesicle behavior by embedding observed uptake patterns into the theoretical constructs of differential geometry, Helfrich elasticity, and curvature-based energetics.

5.1 Asymmetry-Induced Uptake and Spontaneous Curvature

The first major finding of Chapter 4 was that asymmetric vesicles consistently exhibit higher cellular uptake compared to their symmetric counterparts. This observation aligns naturally with the theoretical framework of *spontaneous curvature* introduced in Section 2. As discussed, asymmetry between leaflets leads to a preferred curvature C_0 , and hence a minimized Helfrich bending energy when the vesicle adopts a particular shape.

From the bending energy equation:

$$F_{\text{bend}} = \int_S \frac{\kappa}{2} (2H - C_0)^2 dA, \quad (5.1)$$

we see that energy is minimized when the mean curvature H locally approximates $C_0/2$, as dictated by the minimization of the Helfrich bending energy functional [22]. Vesicles engineered with asymmetric lipid distributions inherently possess a nonzero spontaneous curvature ($C_0 \neq 0$) due to the differential lipid packing, shape, and spontaneous curvature contributions between the inner and outer leaflets [24]. For example, cone-shaped lipids in one leaflet and cylindrical lipids in the other induce a curvature preference toward one side.

As a result, such asymmetric vesicles possess a geometric bias toward bending, even in the absence of external forces. During endocytosis, this pre-existing curvature lowers the energetic threshold for membrane invagination and wrapping, facilitating vesicle internalization by cells.

In contrast, symmetric vesicles (for which $C_0 \approx 0$) have matched curvature contributions from each leaflet, leading to a net zero curvature preference. These vesicles thus require higher thermal or mechanical fluctuations to achieve the curvature necessary for uptake. The use of POPC as the inner leaflet across all asymmetric vesicles standardizes the intrinsic curvature influence, and further isolates the effect of outer leaflet variation.

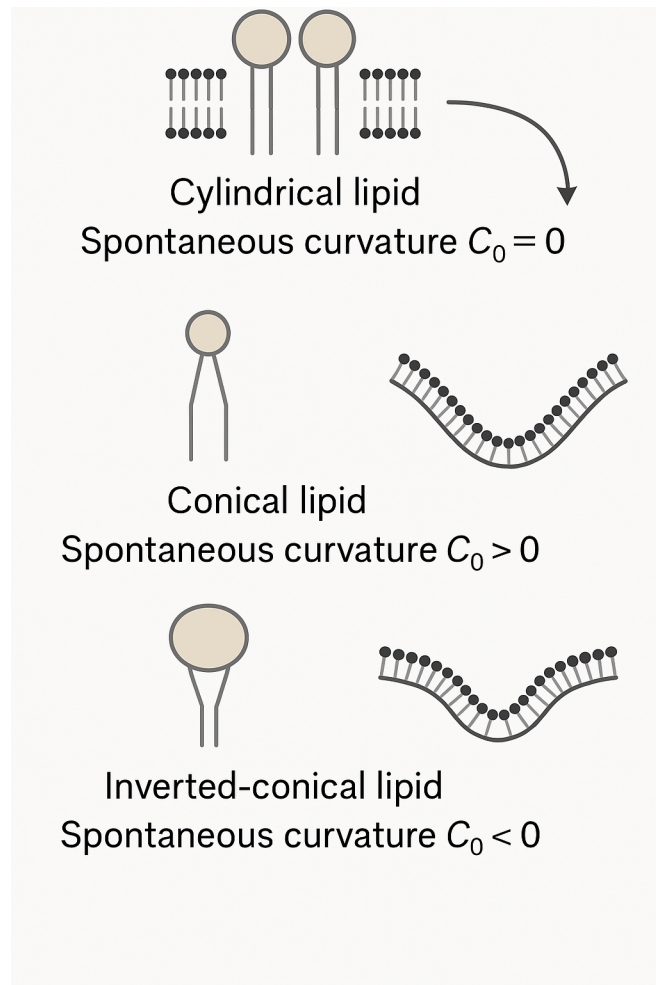


Figure 5.1: Curvature of different lipid structures

This also supports our central hypothesis that vesicle geometry is not merely a byproduct of molecular composition, but a determinant of biological function. Spontaneous curvature emerges as a geometrically interpretable parameter that bridges molecular asymmetry with mechanical behavior, especially in the uptake process.

5.2 Electrostatics and the Effective Bending Modulus

The second major trend—namely that vesicles with large absolute zeta potentials (both positive and negative) exhibit enhanced uptake—can also be interpreted through the lens of the geometric theory. While zeta potential ζ is not explicitly present in the classical Helfrich model [22], we propose an electrostatically modified rigidity model:

$$\kappa_{\text{eff}} = \kappa_0 - \gamma|\zeta|, \quad (5.2)$$

which posits that increased surface charge disrupts lipid packing, reduces bending rigidity κ , and thus promotes membrane deformation.

This mechanism provides a theoretical explanation for the non-monotonic uptake curve observed in Figure 4.3, where vesicles near $\zeta \approx 0$ are poorly taken up. These near-neutral vesicles experience neither strong electrostatic attraction to the negatively charged cell membrane nor sufficient lipid repulsion to induce softening. Consequently, they remain relatively stiff and non-interactive.

Conversely, highly charged vesicles—regardless of charge sign—experience enhanced electrostatic repulsion within the bilayer, lowering κ_{eff} and thereby increasing deformability. This allows the membrane to better conform to cellular invaginations or participate in fusion-like uptake mechanisms. This concept can be understood as follows: in a lipid bilayer, the lipids are packed together like tiles on a flexible surface. When the surface becomes highly charged—whether positively or negatively—the similarly charged lipid headgroups repel each other. This repulsion pushes the lipids slightly apart, decreasing their tight packing. This increased flexibility corresponds to a lower bending modulus κ_{eff} , meaning the membrane can curve more easily.

Additionally, charged vesicles interact more strongly with cell membranes via electrostatic attraction. Since most mammalian cells have negatively charged surfaces, cationic

(positively charged) vesicles are especially prone to adhere and fuse with cells. Surprisingly, even strongly anionic vesicles show improved uptake—likely due to their internal softening and possible involvement in counterion-mediated interactions [37, 38].

Thus, ζ emerges as a dual-purpose modulator: an external interaction vector via surface charge attraction/repulsion, and an internal geometric softener via modulation of effective rigidity.

5.3 Membrane Fluidity, Bending Rigidity, and Curvature Coupling

Membrane fluidity, quantified via Laurdan GP, showed a strong inverse correlation with uptake. Low GP values (high fluidity) corresponded to higher fluorescence intensities, indicating increased delivery. This, too, is consistent with our geometric model. As demonstrated in Chapter 2, GP serves as a proxy for bending rigidity κ , via:

$$\kappa = \kappa_{\max} - \lambda(1 - \text{GP}). \quad (5.3)$$

The interpretation is straightforward: membranes that are more fluid are geometrically softer, possessing lower bending moduli. This enables them to more easily adopt curved configurations, which are necessary for uptake through endocytic wrapping or fusion. Importantly, this trend also supports the empirical curvature-energy hypothesis: *higher uptake corresponds to lower bending energy barriers.*

Further, we hypothesize that fluid membranes facilitate the dynamic redistribution of curvature stress during invagination. Since endocytosis is not a static process but a temporally evolving deformation, the viscoelastic response of the membrane becomes crucial. Fluid membranes can locally accommodate changes in curvature without inducing large energy penalties, which may explain why disordered vesicles outperform more ordered analogs in delivery tasks [39].

This framework also offers an interpretation for the limited performance of highly ordered (gel-phase) vesicles, whose high GP values imply large κ , resulting in rigid vesicles that resist deformation even in the presence of favorable electrostatic conditions.

5.4 Correlated Effects: Toward a Unified Model

Chapter 4 suggested that uptake is not dictated by a single parameter but rather by the confluence of asymmetry, zeta potential, and fluidity. Our correlation matrix (Section 4.4) captures these interdependencies. From a geometric standpoint, all three variables feed into the effective bending energy of the system, either directly through κ , indirectly via C_0 , or through modifications of local tension.

We now propose a composite energy landscape model in which the total energetic cost of deformation is given by:

$$F_{\text{total}} = \int_S \left[\frac{\kappa_{\text{eff}}}{2} (2H - C_0)^2 + \sigma \varepsilon^2(u, v) \right] dA, \quad (5.4)$$

where:

- κ_{eff} depends inversely on both GP and $|\zeta|$,
- C_0 is induced by asymmetry,
- σ and ε reflect induced membrane tension.

Such a model invites future computational simulations: by parametrizing κ_{eff} , C_0 , and σ for each vesicle type, one can theoretically predict uptake probability based on energetic minimization paths, providing a forward model for vesicle design.

This geometric unification enables us to propose a key theoretical insight:

Theoretical Principle

Vesicles with high spontaneous curvature (C_0), low bending rigidity (κ_{eff}), and favorable surface electrostatics exhibit minimized energy barriers for uptake and are thus optimal candidates for drug delivery.

5.5 Perspective

5.5.1 Limitations

While our results have provided interpretive power, several limitations merit attention:

- Our experimental GP and ζ measurements provide system-level averages and may miss local heterogeneities in curvature or charge distribution.
- The assumption of vesicle sphericity in applying curvature models may not fully capture complex morphological transitions during uptake.
- The spontaneous curvature C_0 was not directly measured but inferred; direct shape analysis using cryo-EM or confocal tomography remains a next step.
- The electrostatic softening model remains a theoretical proposition; validating the equation $\kappa_{\text{eff}} = \kappa_0 - \gamma|\zeta|$ requires atomistic or coarse-grained molecular simulations.
- Toxicity and biodistribution profiles were not explored here but are crucial for translational relevance.
- Topological transitions (e.g., fusion, budding) were outside our scope but could become important when vesicle delivery involves endosomal escape or cytosolic release.

5.5.2 Future Direction

Future work on this particular topic should explore:

1. Direct mapping of C_0 via vesicle shape analysis using cryo-EM or confocal tomography,
2. Molecular dynamics simulations to test our proposed relationship $\kappa_{\text{eff}} = \kappa_0 - \gamma|\zeta|$
3. Development of vesicle libraries with orthogonal variations in lipid shape, charge, and fluidity,

4. Machine-learning models trained on energy landscape parameters to predict optimal vesicle formulations,
5. Time-resolved uptake studies to capture kinetic pathways of curvature evolution.

Chapter 6

Conclusion

A poem is never finished, only abandoned

PAUL VALERY

This thesis set out to investigate the design principles, mechanistic underpinnings, and functional performance of lipid vesicles as drug delivery vectors. By integrating high-throughput experimental methodologies with a rigorous biophysical framework rooted in differential geometry and membrane elasticity theory, we have demonstrated how nanoscale vesicle architecture critically influences cellular uptake, a central determinant of delivery efficacy. The results contribute to the growing field of bioinspired nanomedicine by working toward a unified, mechanistic model for vesicle behavior that is both predictive and designable. This geometric-biophysical nexus offers a powerful platform for the rational design of drug delivery vesicles and demonstrates the value of interdisciplinary synthesis in advancing nanomedicine.

6.0.1 Theoretical Unification and Implications

Perhaps the most significant theoretical contribution of this thesis lies in bridging nanoscale molecular asymmetries with macroscopic membrane behaviors using continuum mechanics. By embedding vesicle geometry in the language of differential geometry and elasticity, we have elevated membrane parameters—such as C_0 , κ_{eff} , and σ —from empirical descriptors to tunable design variables.

This allows the field to transition from empirical trial-and-error toward principled engineering. For instance, a vesicle with a high C_0 can be expected to spontaneously invaginate under mild perturbations; a vesicle with low κ_{eff} can conform to cell topography more easily; and a vesicle with optimal surface charge can simultaneously exploit electrostatic attraction and internal softening. These design rules can inform vesicle fabrication protocols tailored to specific delivery contexts—whether the goal is to penetrate dense tissue matrices, target specific cell types, or minimize off-target toxicity.

6.0.2 Broader Context: Toward Universal Drug Delivery Systems

Our findings have practical significance beyond the current experimental scope. Vesicle-mediated delivery platforms are central to next-generation therapeutics, particularly for nucleic acid drugs, CRISPR components, and protein-based payloads. The challenges of delivering large, fragile, or charged molecules to specific intracellular compartments without triggering immune responses or rapid clearance demand delivery vehicles with finely tuned physicochemical and mechanical properties.

Asymmetric lipid vesicles—particularly those optimized via our energetic design framework—may offer a compelling compromise between the stability of synthetic carriers and the efficacy of viral vectors. Unlike viruses, vesicles are non-immunogenic and modular; unlike traditional liposomes, asymmetric vesicles can encode curvature, stiffness, and surface energy in a programmable way. These traits make them attractive candidates for delivering

complex cargos across diverse biological barriers.

6.0.3 Final Remarks

In conclusion, this thesis affirms the central role of symmetry and geometry in vesicle-based drug delivery. Far from being passive containers, lipid vesicles are active mechanical participants whose uptake behavior is encoded in their shape, stiffness, and surface energy. By integrating experimental data with a robust theoretical model, we have moved one step closer to rationally engineering lipid vesicles as customizable vehicles for next-generation therapeutics. The future of drug delivery lies not merely in finding new molecules, but in delivering existing ones better—and geometry, as this work shows, is a powerful guide.

Acknowledgements

It definitely took a village to raise the child that is this thesis, and I am eternally grateful to those that helped me along the way to finally completing it.

To my peers and advisors in the Weitz Lab, this thesis would be nowhere near possible without your active help, support and guidance throughout the process. To Professor Weitz, I am indebted for the opportunity to join this lab for what became the most meaningful academic journey I've had in college, and for always being approachable for any help, advice, or tips on how to continue. To Kevin Jahnke, thank you so much for bringing me into your fold for this project, and allowing me the space and having the confidence within me to work on these novel ideas. Your guidance was much needed to steer the ship and direct where this research needed to be go, every step of the way. To Chenjing Yang, thank you for showing me the ropes on every single method and task in the lab, particularly the vesicle fabrication. Your constant presence and ever willingness to help made it possible for this research to be done on the time scale that it was, and your guidance has taught me so much outside of this research as well. To Alex Yang, thank you for always helping with a smile and being ready to help out with all the vast knowledge that you have.

I also want to thank my advisor, Dr Linsey Moyer, whose guidance across these 4 years steered my concentration, and who was always there to clear my confusions, help me find research opportunities, and give advice on anything and everything Biomedical Engineering.

Appendix A

Experimental Section

Inverted Emulsion / Extrusion Technique

The fabrication process involved the following steps, all conducted under sterile and temperature-controlled conditions:

1. Lipid Film Preparation

- Dissolve 10 µL of a 10 mg/mL lipid solution in chloroform into a 2 mL glass vial.
- Evaporate solvent under a nitrogen stream to form a thin lipid film.
- Desiccate for 15 minutes to remove any residual solvent.

2. Lipid-Oil Solution Formation

- Add 2 mL of mineral oil to the dried film to reach a final concentration of 5 µg/mL.
- Vortex to homogenize and sonicate for 2 hours until clear.

3. Monolayer Preparation

- Add 600 µL PBS into new vials.
- Carefully layer 700 µL of the lipid-oil solution on top.

- Incubate undisturbed for 120 minutes to allow lipid monolayer formation at the oil-water interface.

4. Emulsion Formation and Extrusion

- Mix aqueous cargo (e.g., PBS or fluorescent dye solution) with lipid-oil to create W/O emulsions.
- Transfer to a dual-syringe extrusion apparatus using a 0.2 μm pore-size membrane.
- Extrude 7 times back and forth (odd number) to ensure emulsion homogeneity.

5. Vesicle Formation via Centrifugation

- Carefully add 100 μL of emulsion onto the monolayer interface.
- Centrifuge at 10,000g for 10 minutes.
- Vesicles pass through the interface, forming bilayers and collecting at the bottom aqueous phase.

6. Vesicle Collection

- Preload a syringe with 300 μL PBS.
- Withdraw vesicle-rich bottom phase, being careful to avoid the oil layer.
- Store vesicles on ice or at 4°C prior to analysis.

This technique reliably yields asymmetric vesicles with encapsulated aqueous interior, suitable for both physicochemical characterization and biological assays.

Zeta Potential Measurements

Procedure:

- Vesicle samples were diluted 1:10 in Milli-Q water.
- Measurements were conducted in folded capillary cells at 25°C.
- Each formulation was measured in triplicate.

Confocal Microscopy

Confocal microscopy was performed on a confocal laser scanning microscope (LSM900, LSM980, or SP5) by Zeiss (Carl Zeiss AG) or Leica (Leica GmbH), respectively. The pinhole was set to 1 airy unit, and all experiments were conducted at room temperature. For image acquisition, a 10 \times air (Plan 10 \times /0.22), 20 \times air (Plan-APOCHROMAT 20 \times /0.8 M27), a 40 \times water immersion objective (Plan-APOCHROMAT 40 \times /1.0 DIC M27), and a 63 \times oil immersion (HC PL APO 63 \times /1.40 OIL CS2) were used. Images were analyzed and adjusted in ImageJ. For the analysis of the peripheral and background intensity in Fig. 1D, a custom-written macro was used (49, 50).

Bibliography

- [1] R. Paul, J. Smith, and A. Lee, “Advances in drug development and therapeutics,” *Journal of Medical Chemistry*, vol. 55, no. 4, pp. 1234–1245, 2010.
- [2] T. M. Allen and P. R. Cullis, “Drug delivery systems: From concept to clinical applications,” *Advanced Drug Delivery Reviews*, vol. 65, no. 1, pp. 36–48, 2013.
- [3] M. Pinto, L. Sousa, and J. Costa, “Bioavailability challenges in oral drug administration,” *Pharmaceutics*, vol. 9, no. 2, pp. 45–57, 2017.
- [4] F. Danhier, E. Ansorena, and J. Silva, “Plga-based nanoparticles for drug delivery,” *Journal of Controlled Release*, vol. 161, no. 2, pp. 505–522, 2010.
- [5] V. P. Torchilin, “Liposomal drug delivery systems,” *Nature Reviews Drug Discovery*, vol. 4, no. 2, pp. 145–160, 2014.
- [6] R. Langer, “Polymeric drug delivery systems,” *Science*, vol. 293, no. 5530, pp. 58–60, 1998.
- [7] N. Pattni, V. Chupin, and V. P. Torchilin, “Lipid-based drug carriers,” *Pharmaceutics*, vol. 7, no. 3, pp. 438–463, 2015.
- [8] D. Sercombe, T. Hua, and K. Veedu, “Nanoparticle-based drug formulations,” *Journal of Nanomedicine*, vol. 10, no. 1, pp. 345–357, 2015.
- [9] X. Hou, T. Zaks, R. Langer, and Y. Dong, “Lipid nanoparticles for mrna delivery,” *Nature Reviews Materials*, vol. 6, pp. 1078–1094, 2021.

Bibliography

- [10] R. Tenchov, R. Bird, A. E. Curtze, and Q. Zhou, “Lipid nanoparticles—from liposomes to mrna vaccine delivery, a landscape of research diversity and advancement,” *ACS Nano*, vol. 15, pp. 16982–17015, 2021.
- [11] M. J. Mitchell, M. M. Billingsley, R. M. Haley, M. E. Wechsler, N. A. Peppas, and R. Langer, “Engineering precision nanoparticles for drug delivery,” *Nature Reviews Drug Discovery*, vol. 20, pp. 101–124, 2021.
- [12] E. Blanco, H. Shen, and M. Ferrari, “Principles of nanoparticle design for overcoming biological barriers to drug delivery,” *Nature Biotechnology*, vol. 33, pp. 941–951, 2015.
- [13] V. P. Torchilin, “Recent advances with liposomes as pharmaceutical carriers,” *Nature Reviews Drug Discovery*, vol. 4, pp. 145–160, 2005.
- [14] J. Gubernator, “Active methods of drug loading into liposomes: recent strategies for stable drug entrapment and increased in vivo activity,” *Expert Opinion on Drug Delivery*, vol. 8, pp. 565–580, 2011.
- [15] Y. Elani, S. Purushothaman, P. J. Booth, J. M. Seddon, N. J. Brooks, R. V. Law, and O. Ces, “Measurements of the effect of membrane asymmetry on the mechanical properties of lipid bilayers,” *Chemical Communications*, vol. 51, pp. 6976–6979, 2015.
- [16] C. Yang, J. Menge, N. Zhvania, D. Chen, D. A. Weitz, and K. Jahnke, “Engineering asymmetric nanoscale lipid vesicles for drug delivery,” *bioRxiv*, 2024.
- [17] F. Danhier, E. Ansorena, and J. Silva, “Plga-based nanoparticles for drug delivery,” *Journal of Controlled Release*, vol. 161, no. 2, pp. 505–522, 2012.
- [18] T. Lener, G. Gimona, and L. Aigner, “Extracellular vesicles in drug delivery: Challenges and opportunities,” *Journal of Extracellular Vesicles*, vol. 4, no. 1, pp. 1–12, 2015.
- [19] R. Phillips, J. Kondev, J. Theriot, H. G. Garcia, and N. Orme, *Physical Biology of the Cell*. CRC Press, 2012.

- [20] R. Phillips, J. Kondev, J. Theriot, and H. G. Garcia, *Physical Biology of the Cell*. Garland Science, 2 ed., 2012.
- [21] M. P. do Carmo, *Differential Geometry of Curves and Surfaces*. Prentice-Hall, 1976.
- [22] W. Helfrich, “Elastic properties of lipid bilayers: theory and possible experiments,” *Zeitschrift für Naturforschung C*, vol. 28, no. 11-12, pp. 693–703, 1973.
- [23] D. Boal, *Mechanics of the Cell*. Cambridge University Press, 2 ed., 2012.
- [24] J. Zimmerberg and M. M. Kozlov, “Membrane curvature and deformation by proteins: mechanisms and function in health and disease,” *Nature Reviews Molecular Cell Biology*, vol. 7, no. 1, pp. 9–19, 2006.
- [25] K. Jahnke, M. Pavlovic, W. Xu, A. Chen, T. P. Knowles, L. R. Arriaga, and D. A. Weitz, “Polysaccharide functionalization reduces lipid vesicle stiffness,” *Proceedings of the National Academy of Sciences*, vol. 121, no. 22, p. e2317227121, 2024.
- [26] Z. Leonenko, E. Finot, H. Ma, T. E. S. Dahms, and D. T. Cramb, “Elasticity and phase behavior of dppc membranes modulated by cholesterol: an afm study,” *Biophysical Journal*, vol. 86, no. 6, pp. 3783–3793, 2004.
- [27] E. Evans and W. Rawicz, “Detection of local lipid bilayer curvature and mechanical properties using micropipette aspiration,” *Biophysical Journal*, vol. 58, no. 6, pp. 1201–1207, 1990.
- [28] N. Kučerka, S. Tristram-Nagle, and J. F. Nagle, “Structure of fully hydrated fluid phase lipid bilayers with monounsaturated chains,” *The Journal of Membrane Biology*, vol. 208, no. 3, pp. 193–202, 2005.
- [29] A. J. Verkleij and B. de Kruijff, “Lipid polymorphism and membrane fusion,” *Biochemistry*, vol. 23, no. 23, pp. 5665–5670, 1984.

Bibliography

- [30] J. F. Nagle and S. Tristram-Nagle, “Structure of lipid bilayers,” *Biochimica et Biophysica Acta (BBA)-Reviews on Biomembranes*, vol. 1469, no. 3, pp. 159–195, 2000.
- [31] S. M. Gruner, “The curvature elastic stress of lipid monolayers and membranes,” *The Journal of Physical Chemistry*, vol. 89, no. 8, pp. 1467–1474, 1985.
- [32] M. J. Hope, M. B. Bally, G. Webb, and P. R. Cullis, “Generation of large unilamellar vesicles by a novel method,” *Biochimica et Biophysica Acta (BBA)-Biomembranes*, vol. 812, no. 1, pp. 55–65, 1985.
- [33] S. Pautot, B. J. Friskin, and D. A. Weitz, “Production of unilamellar vesicles using an inverted emulsion,” *Langmuir*, vol. 19, no. 7, pp. 2870–2879, 2003.
- [34] T. Parasassi, G. De Stasio, G. Ravagnan, R. Rusch, and E. Gratton, “Phase fluctuation in phospholipid membranes revealed by laurdan fluorescence,” *Biophysical journal*, vol. 57, no. 6, pp. 1179–1186, 1990.
- [35] Y. Dancik, J. A. Troutman, J. Jaworska, and J. M. Fitzpatrick, “Hepatic uptake and metabolism in drug disposition: What can in vitro models tell us?,” *Current Drug Metabolism*, vol. 16, no. 2, pp. 87–100, 2015.
- [36] S. Knasmüller, V. Mersch-Sundermann, S. Kevekordes, F. Darroudi, W. Huber, C. Hoelzl, J. Bichler, and B. Majer, “Use of human-derived liver cell lines for the detection of environmental and dietary genotoxins; current state of knowledge,” *Toxicology*, vol. 198, no. 1-3, pp. 315–328, 2004.
- [37] J. Li, M. Wu, R. Zhang, X. Chen, C. H. Chan, and X. Sun, “Zeta potential as a modulator of membrane rigidity and endocytic uptake of lipid vesicles,” *Biophysical Journal*, vol. 121, no. 2, pp. 395–406, 2022.

- [38] A. Colom, E. Derivery, S. Soleimanpour, C. Tomba, M. Molin, N. Sakai, M. González-Gaitán, S. Matile, and A. Roux, “Asymmetric cholesterol distribution regulates lipid packing and membrane domains,” *Nature Communications*, vol. 9, no. 1, p. 2049, 2018.
- [39] A. Kusumi, C. Nakada, K. Ritchie, K. Murase, K. Suzuki, H. Murakoshi, R. Kasai, J. Kondo, and T. Fujiwara, “Paradigm shift of the plasma membrane concept from the two-dimensional continuum fluid to the partitioned fluid: high-speed single-molecule tracking of membrane molecules,” *Annual Review of Biophysics and Biomolecular Structure*, vol. 34, pp. 351–378, 2005.